



# Redefining progress, challenges, and future opportunities of mixed-matrix membranes from an engineering perspective for commercial gas separation applications: A review

Yinying Hua <sup>a,1</sup>, Sunghwan Park <sup>\*,b,c,1</sup>, Hae-Kwon Jeong <sup>\*\*, a,d</sup>

<sup>a</sup> Artie McFerrin Department of Chemical Engineering, Texas A&M University, 3122 TAMU, College Station, TX 77843-3122, United States

<sup>b</sup> Department of Energy Chemical Engineering, Kyungpook National University, 2559 Gyeongsang-daero, Sangju-si, Gyeongsangbuk-do 37224, the Republic of Korea

<sup>c</sup> Department of Advanced Science and Technology Convergence, Kyungpook National University, 2559 Gyeongsang-daero, Sangju-si, Gyeongsangbuk-do 37224, the Republic of Korea

<sup>d</sup> Department of Materials Science and Engineering, Texas A&M University, 3122 TAMU, College Station, TX 77843-3122, United States



## ARTICLE INFO

### Keywords:

Mixed-matrix membranes  
Gas separations  
Membrane fabrications  
Engineering perspective  
Scale-up  
Commercialization

## ABSTRACT

Mixed-matrix membranes (MMMs) for gas separations integrate inorganic fillers into a polymer matrix, combining the cost-effective scalability of polymer membranes with the superior performance of expensive inorganic ones. Over the past three decades, the development of MMMs has focused on addressing scientific challenges such as filler agglomeration and poor interfacial interaction, which significantly impact the performance and scalability. Despite breakthroughs in mitigating these issues, translating these achievements into commercially viable solutions has been limited. This review reevaluates the developments, challenges, and prospects of MMMs, emphasizing the engineering perspective in addressing the practical aspects of scale-up and commercialization. It highlights, in particular, fabrication strategies and the importance of engineering approaches in realizing their commercial potential. Furthermore, it discusses the advantages, disadvantages, scalability, and cost implications of both traditional and recent MMM processing methods, outlining the benchmarks required for MMMs to be commercially viable on a large scale. This perspective encourages a shift towards application-driven research to advance the development of MMMs that meet both performance and commercialization criteria.

## 1. Introduction

Increasing attention is being directed towards membrane-based gas separation as a compelling alternative to the current energy-intensive and costly thermally-driven techniques such as distillation [1]. In commercial applications, polymeric membranes have taken a leading role in various gas separations, attributed to their low material costs and ease processing (Fig. 1a). However, polymeric membranes face fundamental limitations in gas separation performance, notably a trade-off between permeability and selectivity, which is crucial for separation performance. Robeson [2] established the upper-bound performance limits of polymer membranes by utilizing the Freeman theory, a

framework combining transition state theory for diffusion and thermodynamics for solubility [3]. In addition, the chemical and thermal robustness of these polymer membranes is concerning. These membranes tend to undergo plasticization when exposed to high-pressure conditions for condensable gases like CO<sub>2</sub>, CH<sub>4</sub>, C<sub>3</sub>H<sub>6</sub>, C<sub>3</sub>H<sub>8</sub>, among others, which adversely affects their gas separation performance [4]. On the other hand, inorganic membranes such as zeolite membranes have undergone intensive study since they are chemically and thermally robust and possess well-defined crystalline structures (Fig. 1b). Due to their tailored molecular sieving properties, some inorganic membranes exhibit exceptional separation performances, notably outperforming polymer membranes and breaking through the traditional

\* Corresponding author at: Department of Energy Chemical Engineering, Kyungpook National University, 2559 Gyeongsang-daero, Sangju-si, Gyeongsangbuk-do 37224, the Republic of Korea.

\*\* Corresponding author at: Artie McFerrin Department of Chemical Engineering, Texas A&M University, 3122 TAMU, College Station, TX 77843-3122, United States.

E-mail addresses: [sunghwan@knu.ac.kr](mailto:sunghwan@knu.ac.kr) (S. Park), [hjeong7@tamu.edu](mailto:hjeong7@tamu.edu) (H.-K. Jeong).

<sup>1</sup> These authors contributed equally to this work.

permeability-selectivity trade-off [5,6]. Nevertheless, the large-scale fabrication of polycrystalline inorganic membranes is limited by their high processing costs, which stem from the complexities in controlling microstructures such as grain boundaries and their inherently fragile mechanical properties [7]. To overcome the limitations of both polymeric and inorganic membranes, mixed-matrix membranes (MMMs), which consist of inorganic fillers dispersed in a continuous polymer matrix, have emerged as a potential breakthrough (Fig. 1c). By incorporating highly selective inorganic molecular sieve fillers into a cost-effective and processable polymer matrix, MMMs aim to balance ease of processing with enhanced gas separation performance, potentially exceeding the upper-bound curves of polymer membranes.

Nonetheless, MMM-based gas separations face several challenges. A critical aspect of MMM processing is the interface between the organic phase and the inorganic filler. The hydrophilic nature of inorganic fillers often leads to poor compatibility with hydrophobic polymers. Consequently, a flawed 'sieve-in-a-cage' morphology may form, acting as a conduit for gas molecule transport [8]. Furthermore, strong inter-filler interactions cause filler agglomeration, leading to mesoporous spaces that allow gas molecules to bypass molecular sieves [9]. The issue of agglomeration worsens when reducing the filler size, a step crucial for creating ultra-thin MMMs. In response to these challenges, numerous researchers have been endeavoring to enhance polymer/filler interactions and filler distribution, aiming to develop scalable and high-performing MMMs through scientific perspectives.

A considerable amount of review articles has highlighted the latest advancements in MMMs for gas separation, offering insights mostly from a scientific standpoint. Dong et al. [10] systematically outlined the primary hurdles facing MMMs, emphasizing crucial scientific strategies for overcoming them. They advocated for optimal pairing of polymers and fillers to improve compatibility and enable potential upscaling. Research into MMMs that incorporate a third component as a compatibilizer has shown promising improvements in interfacial interactions and separation performance, suggesting their viability for large-scale production [11]. Bastani et al. [12] discussed the interfacial morphology between zeolite and polymer in MMMs, modification methods, and thoroughly evaluates the effects of parameters like zeolite loading, pore size, and particle size on gas permeation tests. Additionally, studies thoroughly examined MMMs with noble inorganic fillers, which enhance polymer interactions and offer superior molecular sieving capabilities. Gao et al. [13] reviewed advancements in MXene/polymer membranes, highlighting their properties and applications. Kamble et al. [14] also highlighted the emerging class of inorganic fillers, such as two-dimensional (2D) materials, which have garnered significant attention in recent gas separation research. Guan et al. [15] summarized modifications in zeolitic imidazolate framework (ZIF)-based MMMs aimed at CO<sub>2</sub> separation, while Lin et al. [16] delved into the interfacial morphology between fillers and matrices in metal organic framework (MOF)-based MMMs. Yu et al. [17] investigated advanced characterization techniques to gain a deeper understanding of membrane properties, with a particular emphasis on the MOF-polymer interface as well. To meet industrial needs and overcome commercialization challenges, Goh et al. [18] summarized the latest exploration of MOF-based MMMs designed for harsh operating conditions. Qin et al. [19] introduced the structure and fabrication processes for ternary MMMs in comparison to binary MMMs. They classified different

nanofillers and the third component and provided a detailed summary and analysis of the CO<sub>2</sub> separation performance of the newly developed ternary MMMs. Not only were membrane materials discussed, but also the gas transportation and separation mechanisms in MMMs were extensively covered [20,21]. Moreover, mathematical modeling of MMMs, emphasizing their interactions and interfacial structures, revealed promising prospects and future directions for their application in gas separation [22]. Kim et al. [23] promoted a prospective research direction for MMMs utilizing high-aspect-ratio materials, supported by performance predictions derived from mathematical modeling.

Despite promising advancements, to the best of our knowledge, there have been no reported cases of commercialization and industrial application of MMMs for gas separation, primarily due to complex engineering challenges in current fabrication techniques [24]. Although the scientific approaches have made strides in demonstrating the scalability of MMM technologies for practical industrial use, a notable gap persists between their theoretical potential and actual application. This discrepancy has promoted a shift in our focus from a scientific standpoint to engineering-driven perspectives, aimed at redefining the design and optimization processes of MMM fabrication to bridge these gaps. In this comprehensive review, we reassess the narrative surrounding the progress, challenges, and prospects of MMMs in gas separation through an engineering lens, with a particular emphasis on fabrication strategies. We offer a concise overview of the evolution of MMMs, highlighting key advancements that set the stage for an in-depth analysis of current fabrication methods and their limitations. A detailed evaluation of production costs and scalability provides insights into the potential commercial pathways for MMM technologies. Concluding, we summarize the separation performance of various gas pairs, a factor crucial for the commercial adoption of MMMs, thereby presenting a holistic view of the current and future landscape of the field.

## 2. Chronological progress of MMM

Understanding the chronological development of MMMs is crucial for comprehending both the current state and future trajectories of MMM research. Fig. 2 illustrates a timeline of landmark discoveries in the field. The inception of MMMs for gas separation dates to 1912, when Steinitzer first experimented with embedding minerals into a polymeric rubber to assess CO<sub>2</sub> sorption and permeation. This pioneering work laid the groundwork for the exploration and advancement of MMM technologies [25]. Approximately five decades later, a significant advancement was reported. In 1971, Christen et al. introduced the first MMMs incorporating porous zeolite fillers, specifically mordenite, using polydimethylsiloxane (PDMS) as the continuous polymer phase, for the separation of O<sub>2</sub>/N<sub>2</sub>. This study represented a pivotal moment in the evolution of MMM technologies, broadening their potential applications and setting a new direction for future research [26]. Following this, in 1974, Kemp et al. contributed another significant landmark study by demonstrating the molecular sieve effect of immobilized fillers within silicon rubber/zeolite 5 A MMMs [27]. The researchers elucidated the gas transport mechanism using the dual-mode model and refined the transition-state and steady-state gas permeation theories. The term 'mixed-matrix membrane' was first introduced by Kulprathipanja et al. [28] in 1988 in their patent, which demonstrated enhanced O<sub>2</sub>/N<sub>2</sub> separation efficiency using cellulose acetate (CA)/silicalite-1 MMMs.

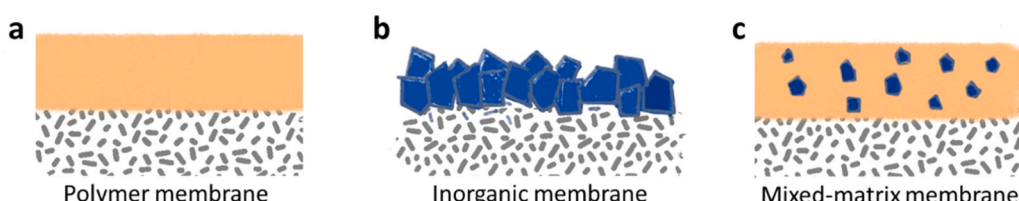


Fig. 1. Illustration of different gas separation membranes.

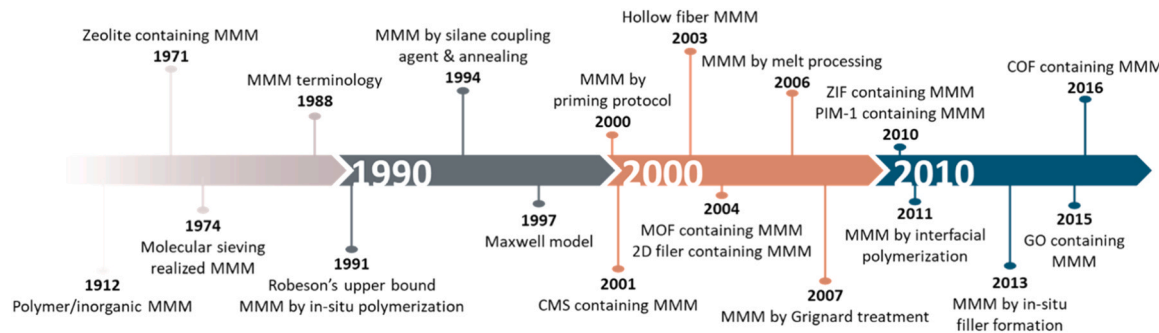


Fig. 2. Timeline of MMM developments.

They also underscored the versatility of MMMs, suggesting a variety of polymers (i.e., polycarbonates (PC), polyamides (PA), polysulfone (PSf), and cellulose acetate (CA)) and fillers including zeolites, silicalites, activated carbons, and ion-exchange resins combinations to engineer MMMs, opening a broad spectrum of potential applications for this technology.

In 1991, the inherent limitations of polymeric membranes were delineated, setting a course for enhancements in MMM separation capabilities [29]. This analysis was further expanded in 2008 to encompass more advanced polymer membranes, such as thermally rearranged (TR) polymers and polymers of intrinsic microporosity (PIMs), indicating a continuous evolution in the understanding and development of membrane technologies [30]. In the same year of 1991, while traditional methods of fabricating MMMs by blending fillers with a PDMS polymer, Jia et al. [31] introduced a revolutionary approach through the in-situ polymerization of PDMS-based MMMs. This method, involving the crosslinking of a cast film embedded with silicalite particles, marked a leap in MMM fabrication by ensuring uniform filler distribution, reducing interfacial voids, and improving the scalability of MMM processing. In 1994, Duval and Mulder et al. [32] unveiled a method to refine the interfacial structure of zeolite/glassy polymer MMMs using silane coupling agents and a thermal annealing process, underscoring the critical role of interfacial engineering in optimizing MMM performance. By 1997, Bouma and Drioli et al [33]. applied the Maxwell model, originally formulated for dielectrics, to predict the gas separation efficiency of MMMs. This interdisciplinary application underscored the versatility and potential of MMMs in gas separation, bridging concepts from different scientific domains to enhance membrane technology. This strong tool is widely accepted even in the current MMM community. In 2000, Mahajan and Koros [34] focused on the complex interactions within the filler-solvent-polymer system. Utilizing this understanding, they managed to achieve a high loading of 40 % in polyvinyl acetate (PVAc)/zeolite 4 A MMMs without interfacial voids through a priming protocol. The following year (2001), carbon molecular sieve (CMS) containing MMM was firstly introduced by Corbin et al. [35]. With increasing attention to MMMs for gas separations, Ekiner et al [36]. prepared the first mixed-matrix hollow fiber membranes (MMHFs) using a dry/wet phase inversion approach in 2003. In 2004, there were the foremost reports of MMMs incorporating two types of fillers attracting considerable interest in the current MMM research. One is MOF-based MMM by Yehia and Musselman et al. [37] and the other is 2-dimensional layered porous material-based MMM by Jeong and Tsatsas et al. [38]. Efforts to enhance polymer-filler adhesion without coupling agents led to the adoption of melt processing techniques in 2006 by Takahashi and Paul [39]. Following this, in 2007, Shu and Koros et al. [40] introduced an alternative method to improve interfacial adhesion in MMMs through Grignard treatment. This technique works by increasing the external surface roughness of inorganic particles, demonstrating the continuous drive towards overcoming interfacial challenges in MMM fabrication.

Over the past decade, the field of MMMs has seen significant

advancements and innovations. A notable development was the introduction of ZIFs, a subclass of MOFs, as fillers in MMMs. Specifically, ZIF-8 and ZIF-90-based MMMs were reported by Musselman et al. [41] and Jones et al. [42], respectively in 2010. These ZIF fillers, renowned for their chemical and thermal stability [43], demonstrated effective molecular sieving capabilities for gas separation and exhibited strong adhesion with the polymer matrix, a trait attributed to their organic linkers. These initial reports ignited widespread interest in ZIF-containing MMMs, a trend continues to this day. In the same year, the first PIM-based MMM was developed by Ahn and Guiver et al. [44]. The high permeability of PIMs has been extensively harnessed, combined with various molecular sieve materials to enhance performance. The year 2011 was marked by another significant achievement when Yu and Wang et al. [45] demonstrated the feasibility of preparing MMMs with sub-micron thickness prepared via interfacial polymerization for gas separation, thereby expanding the application spectrum of MMMs. In 2013, Seoane and Coronas et al [46]. introduced a novel strategy to fabricate MMM of the one-pot in-situ growth of MOF filler in a polymer solution. By 2015, the MMM containing 2D graphene was firstly reported by Li and Wu [47], positioning graphene as a next-generation material for MMMs, as highlighted in many review articles [48–53]. Following closely, in 2016, Kang and Zhao [54] reported MMMs containing covalent organic frameworks (COFs), another promising 2D porous material, thus further diversifying the array of fillers available for cutting-edge gas separation technologies.

Recent advances in MMMs have significantly improved gas separation efficiency through various innovative strategies, focusing on unique material features and design optimizations. Xu et al. [55] developed an ultra-microporous MOF, Cd-MOFs (JLU-MOF87, 88, and 89) with triangular channels, achieving high-efficiency  $C_2H_2/C_2H_4$  separation through a mixed-ligand strategy with different-sized ligands, enhancing  $C_2H_2$  permeability and selectivity in MMMs. Building on MOF potential, Eddaoudi and his co-workers [56] introduced the fluorinated MOF AlFFIVE-1-Ni, tailored into nanosheets and aligned to form a [001]-oriented membrane, demonstrating exceptional hydrogen sulfide and carbon dioxide separation from natural gas, highlighting structural alignment's effectiveness. Chung's group [57], focusing on preventing discrete nanofiller phases with soluble organic macrocyclic cavitands (OMCs), achieved outstanding high-temperature  $H_2/CO_2$  separation, emphasizing phase homogeneity's importance. Tan et al. [58] leveraged high-loading nanofillers by integrating  $CO_2$ -philic Na-SSZ-39 zeolite with polyimide, achieving a remarkable  $CO_2/CH_4$  selectivity of 423 and  $CO_2$  permeability of 8300 Barrer through ultrahigh zeolite loadings and a gas-percolation pathway, showcasing high aspect ratio fillers' potential. Similarly, Hu et al. [59] demonstrated the critical role of nanofiller shape in MMMs by using branched palladium (Pd) nanorods (NRs) in polybenzimidazole, significantly reducing loading requirements while enhancing  $H_2/CO_2$  separation. Pd NRs in polybenzimidazole (PBI) at 3.9 vol% achieved 110 Barrer  $H_2$  permeability and 31  $H_2/CO_2$  selectivity at 200°C, surpassing Robeson's upper bound. These advancements underscore the importance of material design, alignment/distribution,

and shape optimization of fillers in enhancing MMM performance in gas separation applications.

### 3. Type of MMMs

It is essential to optimize gas separation membranes for commercial use. At the core of this optimization is the membrane module, the fundamental unit where individual membranes (either flat sheets or hollow fibers) are assembled for large scale practical applications. The efficiency of gas separation significantly depends on the type of membrane module employed. In general, there are two categories of membranes: flat sheet and tubular-type membranes. Flat sheet MMMs can be configured into plate-frame module MMMs (PF-MMMs) and spiral-wound module MMMs (SW-MMMs), as depicted in Fig. 3a. On the other hand, mixed-matrix hollow fiber membranes (MMHFs) exemplify tubular-type MMMs, with their modular counterpart being hollow-fiber module MMMs (HF-MMMs), illustrated in Fig. 3b. From an engineering perspective, the commercial viability of MMM modules hinges on several factors, including the cost of module fabrication and maintenance, packing density, surface-area-to-volume ratio, and application scope. The advantages and disadvantages associated with different types of membrane modules have been comprehensively reviewed by Mubashir and Fong et al. [60], offering valuable insights for the development of commercial MMM products as outlined in Table 1.

#### 3.1. Flat sheet MMMs: PF-MMMs and SW-MMMs

PF-MMMs have been favored for decades due to their straightforward fabrication processes, low pressure drops and energy-efficient operation [60]. Various fillers have been incorporated into different polymeric matrix to form PF-MMMs for diverse gas separation system. Examples include carbon nanotubes/polyimide (PI) for CO<sub>2</sub>/CH<sub>4</sub> [61], ZIF-8/PEBAX for CO<sub>2</sub>/N<sub>2</sub> [62], organoclay/ polysulfone (PSf) for O<sub>2</sub>/N<sub>2</sub> [63], ZIF-8/6FDA-DAM for C<sub>3</sub>H<sub>6</sub>/C<sub>3</sub>H<sub>8</sub> [64] and so on [65–67]. These inorganic fillers improved the properties and gas separation performance. For instance, asymmetric PF-MMMs with a low loading of nano-sized ZIF-8 (up to 1 wt%) fillers in PSf were fabricated by a dry/wet phase inversion approach [68]. Compared to the neat polymeric membrane, these PF-MMMs showed enhanced CO<sub>2</sub> permeability and CO<sub>2</sub>/CH<sub>4</sub> selectivity [68]. At a 0.5 wt% ZIF-8 filler loading, CO<sub>2</sub> permeability increased by 37 % (from 21.27 GPU to 29.22 GPU) and CO<sub>2</sub>/CH<sub>4</sub> selectivity enhanced by 19 % (from 19.43 to 23.16) [68]. Additionally, significant improvements in thermal and mechanical stability were observed even at a 0.25 wt% ZIF-8 loading [68].

SW-MMMs consist of two flat sheet MMMs separated by a spacer, with a central hollow for collecting permeated gas molecules. Compared to PF-MMMs, SW-MMMs exhibit higher packing density, increased pressure drops, lower cost per membrane area, and greater surface area relative to volume (see Table 1). Despite these advantages, both SW-MMMs and PF-MMMs require substantial operation spec. A notable drawback of SW-MMMs is their difficulty in cleaning, indicating that their maintenance could be challenging.

#### 3.2. Tubular-type MMMs: HF-MMMs

HF-MMMs are distinguished by their highest packing density and most advantageous surface-area-to-volume ratio, along with the lowest production costs per membrane area among their counterparts, PF-

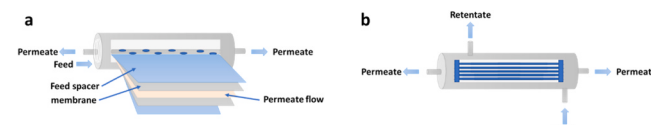


Fig. 3. Illustration of SW-MMM (a) and HF-MMM (b).

Table 1

Comparison of different membrane modules for gas separation [60]. Copyright 2018, Wiley.

Property	Membrane geometry		
	PF-MMM	SW-MMM	HF-MMM
Manufacturing cost (USD m <sup>-2</sup> )	100–200	30–100	5–20
Packing density	Low	Low	High
Pressure drop	Low	High	Low
Suitability for high pressure	Yes	Yes	Yes
Surface area per unit volume	Low	High	High
Space required	Large	Large	Small

MMMs and SW-MMMs. These characteristics make HF-MMMs particularly attractive for commercial applications in the realm of MMM modules. However, despite these significant advantages, HF-MMMs often have a relatively low pressure tolerance and pose more challenges in terms of repairs compared to other MMM modules [60]. The manufacturing processes for hollow fiber membranes are also more complex and demanding than those for flat sheet membranes due to their unique geometrical characteristics. Several laboratory-scale studies have underscored the potential for superior gas separation performance in HF-MMMs. Zahri et al. [69] reported HF-MMMs containing graphene oxide and PSf for CO<sub>2</sub> separation. With just a 0.25 % graphene oxide (GO) loading, the CO<sub>2</sub> permeability of HF-MMMs reached 74.47 GPU and the CO<sub>2</sub>/N<sub>2</sub> selectivity was 44.4, representing 14 % and 158 % enhancements, respectively. Similarly, Liu et al. [70] embedded Y-fum-fcu-MOF into 6FDA-DAM to fabricate HF-MMMs for the removal of CO<sub>2</sub> and H<sub>2</sub>S from natural gas. Uniformly thin (~300 nm) and defect-free membranes, incorporating nanosized (~60 nm) ZIF-8 fillers within a PBI matrix, were developed by Etxeberria-Benavides et al. [71] to effectively treat pre-combustion and syngas streams under high temperature (150 °C) and pressure (up to 30 bar) conditions. Pazani et al. [72] presented a thorough and up-to-date overview of the advancements in mixed matrix hollow fiber composite membranes (MM-HFCMs) for practical CO<sub>2</sub> separation applications. Despite the promising results, the predominant form of reported MMMs has been flat sheet rather than hollow fiber. This is likely due to the challenges associated with managing skin layer imperfections and the polymer/filler microstructures in MMHFs using conventional MMM fabrication techniques [49,73,74].

### 4. MMM fabrication strategies

#### 4.1. Solution processing

Solution processing is the most traditional and widely employed method for fabricating MMMs through blending, favored for its simplicity. This method primarily used to create flat sheet membranes on a laboratory scale, with relatively few applications to MMHFs. The typical steps in solution processing involve (1) preparing a polymer/filler dope solution through blending, (2) casting the solution into the desired size and thickness, (3) solidifying the MMM through solvent evaporation, and (4) thoroughly drying the resulting film [16,75].

Fig. 4 illustrates three common methods for preparing filler-suspended mixed-matrix dope solutions. The first approach involves mixing fillers into a polymer solution, which is prepared by fully dissolving a polymer in a suitable solvent (Fig. 4a). An alternative method involves dispersing inorganic fillers uniformly in a solvent, followed by dissolving a polymer in the prepared filler suspension (Fig. 4b). A third approach separately prepares a polymer solution and a filler suspension, which are subsequently mixed (route c, Fig. 4c). Selecting the appropriate solvent is crucial for the successful fabrication of MMMs, considering factors such as the polymer's solubility, the solvent's volatility, boiling point, and its interaction with fillers. The solvent's interaction with fillers is, in particular, important, as highlighted by Koros

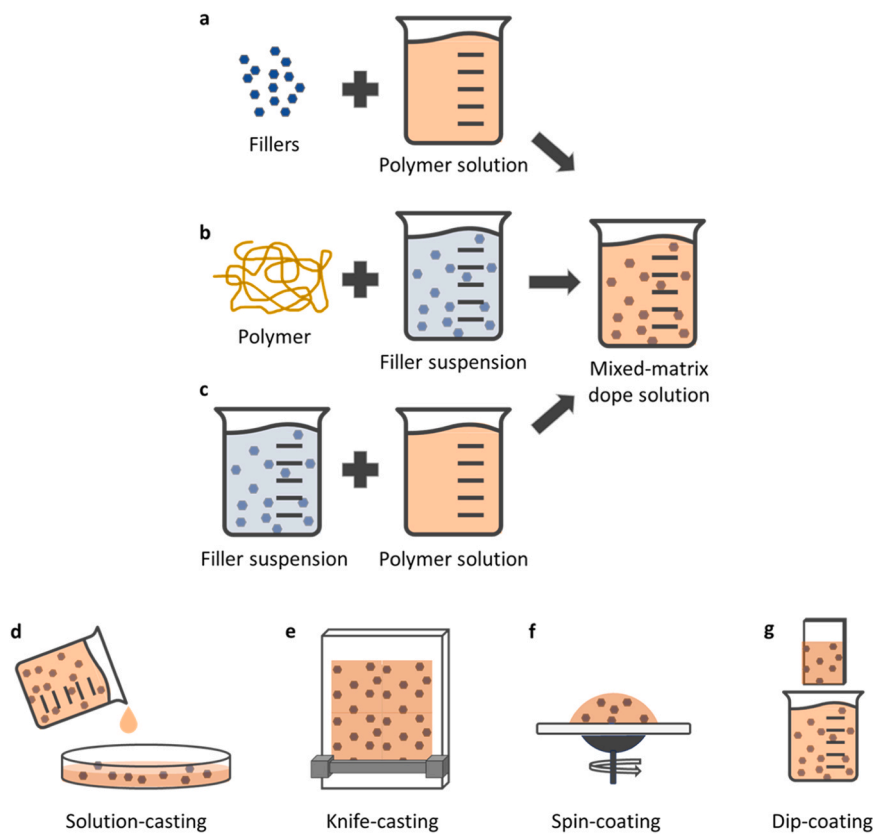


**Fig. 4.** Illustration of different routes for mixed-matrix dope solution preparations (a-c); illustration of MMM fabrication methods using solution processing (d-g).

et al. based on the three-component interaction theory, playing a vital role in the development of effective MMMs [34,76]. Proper solvent-filler interaction is key to preventing filler agglomeration and sedimentation, while also enhancing adhesion between fillers and the polymer matrix [76,77]. A priming protocol based on the three-component interaction theory was developed to improve the wettability of fillers by the polymer solution, involving the dissolution of a portion of the polymer in a filler suspension [34]. Furthermore, achieving a uniform dispersion of fillers within the suspension may require external forces, such as high shear mixing or ultrasonication. However, overly aggressive homogenization can lead to break down fillers or trigger Ostwald ripening [78]. Consequently, it is important to apply appropriate techniques for dispersing fillers to ensure optimal results.

The thickness and uniformity of MMMs produced through solution processing can vary widely from several micrometers to a few nanometers, influenced by the chosen casting method and its specific parameters. Four prominent methods for casting MMMs are solution-casting, knife-casting, spin-coating, and dip-coating. These techniques are outlined and compared in Table 2, demonstrating the array of approaches available for fabricating MMMs. It is notable that the methods employed for casting MMMs closely resemble those for polymer membranes, indicating consistency in fabrication techniques across different membrane types. Detailed descriptions of each casting method can be

found in previous review papers focused on polymer membranes [79].

Solution-casting, also known as drop-casting, is particularly favored for its traditional and straightforward approach within the realm of solution processing, as illustrated in Fig. 4d. Its widespread use is attributed to its simplicity and effectiveness in fabricating membranes [32,80]. The solution-casting method involves (1) depositing a mixed-matrix dope solution onto a casting mold, such as a ring or plate; (2) evenly spreading the solution across the mold; (3) allowing the solvent to evaporate, resulting in solidified MMMs. Diluting the dope solution with solvent is beneficial for reducing viscosity and ensuring smooth spreading, although it may prolong solvent evaporation and potentially lead to filler sedimentation. When solution-casting on a porous substrate, a very thin gutter layer may be necessary to prevent the diluted dope solution from penetrating the porous layer. The thickness of MMM can be adjusted by varying the solution concentration ([polymer + filler]/[polymer + filler + solvent]), the mold dimensions, and the solvent density. Achieving an ultra-thin (<1 μm) and defect-free uniform thickness, however, remains challenging with this technique.

Conversely, knife-casting (also known as doctor blade or tape-casting) enables the achievement of more consistent thicknesses through the mechanical action of the dope solution being pushed through the gap between a substrate and a casting knife, as shown in Fig. 4e. To produce even thinner and more uniform MMMs, spin-coating serves as an alternative. This method distributes the dope solution across the substrate using centrifugal force generated by spinning the substrate, as depicted in Fig. 4f. The spinning rate and the concentration of the dope solution are critical factors in determining the final thickness of MMMs [81]. An additional benefit of spin coating, compared to other methods, is its efficiency in time-saving, as solvent evaporation takes place concurrently with the spinning action. Despite the simplicity and cost-effectiveness of solution processing techniques, they are generally batch processes, which may limit the ability to rapidly produce MMMs on a large scale. Knife-casting as well as spin-coating techniques can be

**Table 2**

Comparisons of different casting techniques.

Casting method	Thickness	Uniformity	Time	Simplicity	Continuity
Solution-casting	Moderate	Low	Slow	Very high	Low
Knife-casting	Moderate	High	Moderate	Very High	Moderate
Spin-coating	Very thin	High	Fast	High	Low
Dip-coating	Thin	Moderate	Fast	High	High

adapted to produce PF- and SW-MMMs.

On the other hand, dip-coating (illustrated in Fig. 4g) stands out as one of the few methods that allows for continuous fabrication of MMHFs within the solution-based processing approaches. However, it is noteworthy that the majority of studies employing dip-coating for MMM production have focused on flat sheet membranes, rather than hollow fibers [82]. A more in-depth exploration of how MMHFs benefit from dip-coating is covered in Section 5 & 6. To regulate the thickness of MMMs during the dip-coating process, factors such as the rate of immersion and withdrawing, dwelling time, and the number of cycles need to be considered [83]. Besides, there are less common methodologies involving solution processing such as spray coating [84] and slot die coating [85].

Furthermore, solvent evaporation significantly impacts the formation of uniform and defect-free MMMs during solution processing. Rapid solvent evaporation can lead to wrinkling, surface unevenness, and pinholes [86]. Other factors such as humidity, atmospheric conditions, and temperature also play a considerable role in the solidification of polymers. Given these, control of the rate of solvent evaporation is crucial in the fabrication of MMMs. Solvents can be classified into two main categories based on their volatility. For example, dichloromethane (DCM), chloroform, acetone, and tetrahydrofuran (THF) are commonly used volatile solvents, while N,N-dimethylacetamide (DMAc), N,N-Dimethylformamide (DMF), and 1-Methyl-2-pyrrolidone (NMP) are the common non-volatile solvents for MMM fabrication [87]. Casting dope solutions in a solvent-saturated chamber is an effective way to slow down the evaporation rates of volatile solvents and to maintain low humidity [88]. For the non-volatile solvents, MMMs have been successfully fabricated under heating and/or vacuum conditions with a gradual increase in temperature [89].

#### 4.2. Melt processing

Compared to solution processing, melt processing offers several advantages: it is faster, more conducive to continuous, and notably more economical and environmentally friendly. This is because of the absence of toxic organic solvent during the process, eliminating the need for solvent recycling. Melt processing for fabricating MMMs involves four steps: (1) Solid polymers are melt into liquids by increasing temperature. (2) The molten polymer is blended with fillers using extruder, internal mixer, or two-roll mill under either gravity or external pressure. (3) The molten polymer containing homogeneously dispersed fillers is cast into molds of desired shapes. (4) The cast liquid is solidified into MMMs by cooling [90]. Micropores in membranes produced by melt processing can be generated by cold-stretching [91,92] and salt-leaching [93].

Although there have been relatively few studies on using melt processing for gas separations, some research highlights its potential. Razaz et al. [94] incorporated nano-sized zeolite 5 A into linear low-density polyethylene (LLDPE)/low-density polyethylene (LDPE) blend to form MMHFs through continuous melt extrusions using a twin-screw extruder coupled with a calendering system (Fig. 5). With up to 20 wt% zeolite 5 A, the gas separation performance of these MMHFs was enhanced compared to that of neat polymer membranes. Similarly, Covarrubias et al. [95] demonstrated the significantly increase in gas separation performances of polyethylene (PE)/porous layered aluminophosphate (ALPO) MMMs prepared by melt compounding. The ALPO swollen by cetyltrimethylammonium (CTA) formed the intercalated structure, resulting in an effective gas transport pathway and reduced PE crystal sizes. However, Kathuria et al. [96] pointed out the limitations of melt compounding for MMM fabrication. For the case of poly(L-lactic acid) (PLLA)/water saturated HKUST-1 MMMs, the crystal structure of HKUST-1 fillers was changed and the PLLA polymer degraded by the high temperature upon the melt processing. Likewise, the chemical modification of graphene incorporated in MMMs was damaged during melt processing [97]. Furthermore, melt processing is limited to semi-crystalline thermoplastic polymer-based MMMs. Since the crystalline phase of these polymers is mostly impermeable to gas molecules, MMMs prepared by melt processing are suitable for gas barriers rather than gas separations [98].

For developing MMMs for gas barriers by melt processing, a variety of non-porous fillers including clay [99,100], silica [101], graphene [102–105], and layered silicate [106,107] have been incorporated into semi-crystalline polymers. Especially, fillers with 2D sheet-like morphology remarkably increase the tortuosity of the gas molecule diffusion pathway due to their high aspect-ratio, effectively improving the gas barrier properties of MMMs [99,100,102–104,107]. As such, the distribution of these fillers, whether through exfoliation or intercalation, is of critical importance for improving gas barrier efficiency. Adak et al. [99] prepared polyurethane/nanoclay MMMs as gas barriers through melt extrusion, comparing direct mixing to master-batch mixing where nanoclays are pre-dispersed in a solvent. The master-batch mixing, which allowed for the exfoliation of nanoclays, showed ca. 30 % improvement in gas barrier properties due to increased tortuosity in the gas diffusion pathway. Consequently, to avoid filler agglomeration, the optimal filler loading of in MMMs is typically less than 5 wt% [99,100,104,108].

#### 4.3. Phase inversion

For the commercial applications of gas separation membranes, it is of

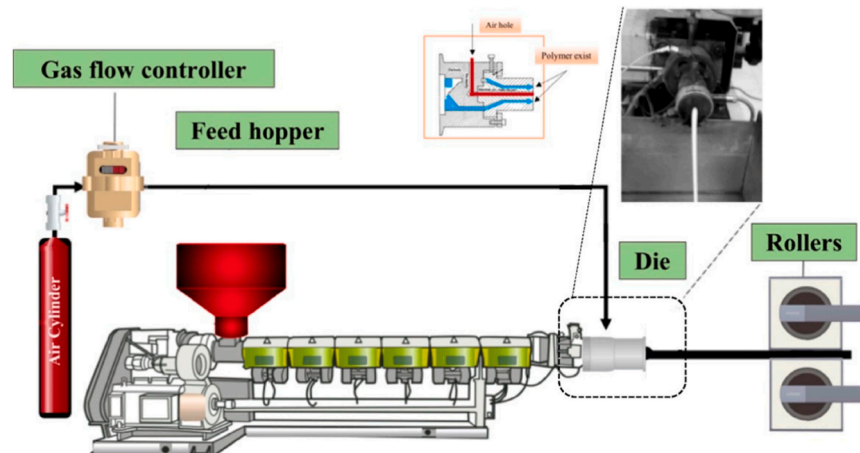


**Fig. 5.** Schematic representation of the extrusion set-up to produce hollow fiber mixed matrix foamed membranes [94]. Copyright 2018, Multidisciplinary Digital Publishing Institute.

critical importance to achieve a dense selective skin layer in the scale of a few hindered nanometers without defects for high productivity. The thin skin layer should be supported by a relatively thick porous support layer (i.e.,  $> \sim 100 \mu\text{m}$ ) to withstand the transmembrane pressure, the driving force of gas transfer across membranes, while minimizing mass transport resistances. As such, an asymmetric structure is preferred for commercial gas separation membranes. The phase inversion process is an effective means to form asymmetric structures in polymeric materials. It is, therefore, widely used for commercial polymeric membrane fabrications. This technique has also been applied to MMMs, resulting in diverse asymmetric MMMs.

The key of the phase inversion process lies in selecting appropriate polymer/solvent/non-solvent system, which can be detailed by a ternary phase diagram [109]. The process involves immersing a cast or spun dope solution into a non-solvent coagulation bath, where it solidifies into a membrane via liquid (solvent)-liquid (non-solvent) demixing process. The morphologies of membranes are determined by ratios and rates of demixing process. A sponge-like membrane morphology is formed when the demixing rate is slow by the low miscibility of solvent with the non-solvent. Otherwise, a finger-like morphology shows up. In the context of MMMs, the demixing process can be influenced by dispersed fillers in the dope solutions. For instance, the hydrophilic HSSZ-13 zeolite dispersed in a mixed-matrix dope solution enables to locally accelerate demixing rates with water, leading to low polymer concentrations around the zeolite and the formation of interfacial voids [110].

There are several challenges of commercially available MMM fabrications using phase inversion. The presence of fillers in the dope solution can generate defects in membrane skin layers, not only through pinholes but also via polymer/filler interfacial voids and filler agglomerations. Considering the manufacturing costs, the support layer could be made from an inexpensive polymer with fillers only present in the skin layer, leading to MMHFs typically having a dual-layer asymmetric structure. This structure comprises a mixed-matrix shell with a thin skin layer and a core of a porous support layer made from economical polymer [111]. However, achieving a defect-free skin layer is more challenging in a dual-layer spinning process compared to single-layer spinning due to different phase inversion conditions for shell and core layers. Furthermore, high filler loadings in MMMs are constrained by processing factors; for MMHFs, high filler contents can increase the viscosity and decrease the elasticity of the mixed-matrix dope solution, adversely affecting its spinnability [111].

#### 4.3.1. Wet spinning

In the wet spinning process, the outer layer of asymmetric MMHFs solidifies immediately upon contact with the coagulant bath without air gap (Fig. 6a). Increasing the air gap can lead more defects due to greater elongation and gravitational stress [112]. A dual-layer polyethersulfone (PES)/P84 asymmetric MMHFs containing PES-zeolite beta was fabricated through the wet spinning process [113]. The outer layer of the MMHFs exhibited fewer defects compared to MMHFs spun with a 1.5 cm air gap. The presence of PES-zeolite beta positively influenced both pure and mixed gas separation tests.

#### 4.3.2. Dry-wet spinning

The dry-wet spinning involves nascent filaments passing through an air gap, during which solvent evaporation and partial phase inversion occur at the interfaces of air/outer dope and inner dope/bore fluid, respectively (Fig. 6b). A larger air gap results in a longer exposure to air, leading to a thicker dense layer. To explore the influence of incorporation of inorganic particles into the phase inversion process, asymmetric MMHFs based on MIL-53 were fabricated by dry-wet spinning process [114]. The MMHFs showed that MIL-53, when grouped with EtOH as a non-solvent, significantly affected the phase inversion process. With 5 wt% MIL-53 loading, the MMHFM demonstrated enhanced gas separation performance with  $\text{CO}_2$  and  $\text{O}_2$  permeability increasing by 129 % and 138 %, respectively, compared to a neat Ultem hollow fiber membrane, while the selectivity of  $\text{O}_2/\text{N}_2$  and  $\text{CO}_2/\text{CH}_4$  remained unchanged.

#### 4.4. In-situ approach

Recently, in-situ bottom-up approaches have garnered significant interest from MMM researchers as promising strategies to overcome MMM challenges (i.e., polymer/filler adhesion and filler dispersion). Their flexibility and scalability provide great potential for the development of advanced MMMs for gas separations. The in-situ approach is primarily divided into in-situ polymerization and in-situ filler formation [115]. In in-situ polymerization methods, polymer precursors (i.e., monomers, oligomers, solvent, and/or additives including crosslinker or polymerization initiator) are blended with filler particles and then sequent polymerization occurs via in-situ manner. This process encompasses in-situ crosslinking, post-synthetic polymerization, and interfacial polymerization. In contrast, in-situ filler formation methods involve growing filler crystals either within the cast dope solutions or inside the solidified polymer membranes.

##### 4.4.1. In-situ polymerization

**4.4.1.1. In-situ crosslinking.** Despite the recent attention on in-situ polymerization, conventional in-situ crosslinking-based MMM fabrications has been used since the early 1990s [116,117]. One of the primary applications of in-situ crosslinking was blending silicone rubber precursors with silicalite-1 zeolite fillers followed by in-situ crosslinking upon film formation [31]. Taking the advantages of the in-situ polymerization approach and the flexibility of polymer chains, the filler loading was reached up to 70 wt% without defects. The as-synthesized MMMs showed improved permeability for  $\text{He}$ ,  $\text{H}_2$ ,  $\text{CO}_2$ , and  $\text{O}_2$  along with selectivity from 2.14 and 11.6–2.92 and 17.1 for  $\text{O}_2/\text{N}_2$  and  $\text{CO}_2/\text{N}_2$  separations, respectively. In a more recent MMM, Ma et al. [117] prepared poly(PEGMA-co-PEGDMA)/UiO-66 type MOF MMMs by in-situ crosslinking PEG containing monomers, poly(ethylene glycol) methacrylate (PEGMA) and poly(ethylene glycol) dimethacrylate (PEGDMA) (Fig. 7a). The  $\text{CO}_2/\text{CH}_4$  separation performance of the membranes was enhanced by incorporating filler loading up to 35 wt%.

**4.4.1.2. Interfacial polymerization.** Interfacial polymerization (IP) emerges as a promising fabrication strategy to commercialize MMMs. IP is utilized to rapidly synthesize an ultrathin polymer layer at the interface between two separated phases (i.e., aqueous and organic phase) [119]. This technique gives rise to thin film composite (TFC) membranes (i.e., polymer membranes) and allows for preparing thin film nanocomposite (TFN) membranes (i.e., MMMs) by incorporating fillers during the IP process. Generally, these membranes are characterized by their ultrathin nature with thicknesses of a few hundred nanometers on porous substrates [120]. Although highly scalable, currently, its applications has predominantly been in liquid separations rather than gas separations. This is likely due to the defects on the ultrathin layers [120]. Nonetheless, there have been a few reports claiming that TFNs

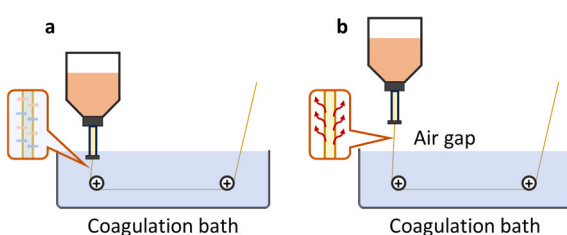
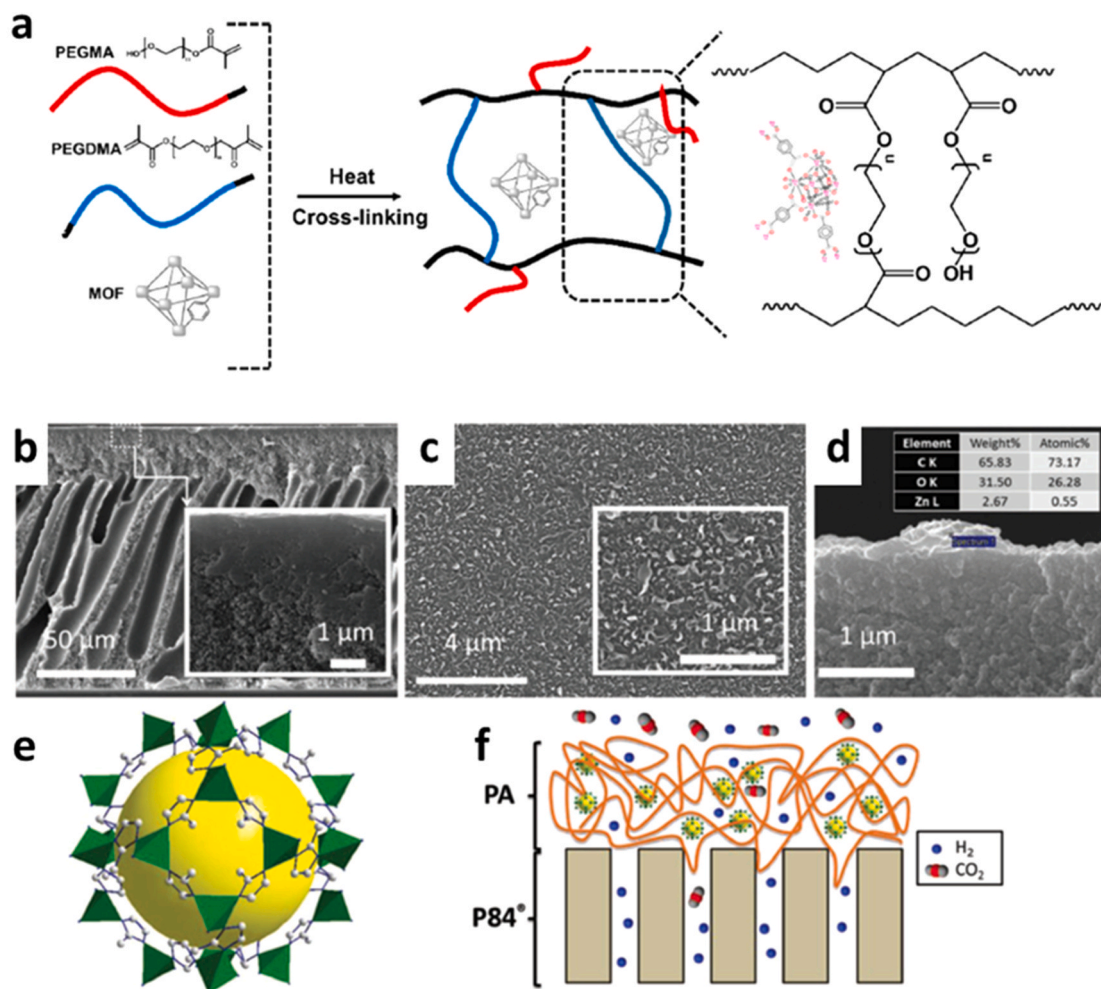


Fig. 6. Illustration of hollow fiber membrane fabrication by wet-spinning (a) and dry-wet spinning (b).



**Fig. 7.** Schematic Illustration of the synthetic approach for the preparation of MMMs based on cross-linked poly[(ethylene glycol) methacrylate] and MOF (a)[117]. Copyright 2018, American Chemical Society. SEM characterization of TFCs & TFNs prepared on polyimide P84® support. (b) Image of the cross-section of a TFC with an inset at higher magnification. (c) Image of the surface of the TFC with a zoom as inset. (d) EDX analysis of a TFN containing a 0.8 % w/v of ZIF-8. Schematic representations of (e) ZIF-8 and (f) the TFN membrane[118]. Copyright 2018, Wiley.

were used as gas separation membranes [45,118,121–123].

The control of pinhole formation during IP with filler incorporation is of critical importance for the utilization of TFNs as gas separation membranes. Wong and Goh et al[122]. developed a TFN using PEO-based polyamide with carbon nanotube (CNT) fillers functionalized with PMMA for CO<sub>2</sub> separations. The PMMA grafting enhanced the dispersion and adhesion of CNT fillers, albeit with some sacrifice in gas selectivity due to uncovered polyamide areas. On the other hand, the polyamide/carbide-derived-carbon (CDC) TFNs prepared by IP for gas separation were reported by Awad and Aljundi [123]. Forming the layer-by-layer structure of polyamide film by multi-cycle of IP, the CO<sub>2</sub>/CH<sub>4</sub> selectivity of polyamide/CDC TFNs increased from ~20 to ~24 resulting from the sealing of pinholes. However, as a consequence, the increase in membrane thickness compromised the CO<sub>2</sub> permeance by ~ 43 %.

Besides from the carbon-based TFN studies, TFNs combining ZIF-based fillers have been developed, contributing to the integrity of polyamide layers. Sánchez-Laínez and Coronas et al[118]. demonstrated the effectiveness of TFNs by IP for gas separations using ZIF-8 as a filler. The synthesized TFN had a thickness ranging from 50 to 100 nm and it contained ZIF-8 particles of 30 nm in size with filler loadings of 0.2 ~ 0.8 % w/v (Fig. 7b-f). It was pointed out that the amount of ZIF-8 required to fabricate TFNs by using IP was substantially lower than that of MMMs using other fabrication strategies. The TFN showed

increased H<sub>2</sub>/CO<sub>2</sub> selectivity and decreased H<sub>2</sub> permeance relative to those of the TFC, affirming the integrity of polyamide layer in the TFN. Nevertheless, due to the filler agglomeration, the optimal ZIF-8 loading was relatively small (i.e., 0.4 w/v). To enhance the compatibility and dispersion of fillers, Yu and Liu et al. [121] prepared TFNs via IP using amine-functionalized ZIF-8 fillers. The amine-functional groups on ZIF-8 fillers formed covalent bonds and hydrogen bonds with the organic phase monomers and the aqueous phase monomers, respectively. As a result, the optimal filler loading of TFN was ~ 1.0 w/v, showing 228 % and 106 % increase in CO<sub>2</sub> permeance and CO<sub>2</sub>/N<sub>2</sub> selectivity, respectively, in comparison with that of the corresponding TFC.

**4.4.1.3. Post-synthetic polymerization.** The post-synthetic polymerization (PSP), also known as the grafting-from approach, represents an in-situ polymerization technique from a solid surface [79], resembling in-situ crosslinking as both methods employ in-situ polymerization by crosslinking small molecules blended with fillers. However, PSP differs from in-situ crosslinking through the functionalization of filler surfaces with polymerizable functional groups that form strong covalent bonds with oligomers [115]. The functionalization allows for the copolymerization of monomers and fillers. Due to the interconnection of oligomer and filler by chemical bonds, the MMMs fabricated by PSP displayed significantly enhanced particle dispersion and adhesion between the polymer and fillers compared to that of in-situ crosslinking [124–126].

A novel strategy to fabricate MMMs with covalently linked fillers and polymers by photoinduced PSP was demonstrated by Feng and Wang et al. [127]. Initially, UiO-66-NH<sub>2</sub> fillers were functionalized with vinyl groups (Fig. 8a). The subsequent in-situ copolymerization of vinyl functionalized UiO-66-NH<sub>2</sub> fillers and butyl methacrylate monomers was performed under UV irradiation (Fig. 8a). This approach resulted in the formation of crack-free MMMs with uniform filler distribution. Similarly, Molavi and Shojaei et al. [124] employed vinyl functionalized UiO-66 induced in-situ copolymerization, achieving a high degree of grafting between poly methyl methacrylate (PMMA) and UiO-66. The high degree of grafting provided stronger interfacial adhesion and more uniform filler distribution, resulting in MMMs with superior selectivity.

Applying PSP to glassy polymers with high fractional free volumes is particularly intriguing for achieving high gas separation performances with the improved MMM microstructure. Cadmium (Cd)-based MOF fillers synthesized from hexafluoroisopropylidene diphthalic anhydride (6FDA) as an organic ligand, were introduced to the in-situ copolymerization of 6FDA and oxydianiline (ODA) monomers, producing grafted 6FDA-ODA/Cd-6FDA MMMs (Fig. 8b) [125]. The covalent bonds formed between the COO<sup>-</sup> group of Cd-6FDA filler surface and the NH<sub>2</sub> group of ODA monomer significantly enhanced the polymer/filler interface. As such, the MMMs showed exhibited 4 times higher CO<sub>2</sub>/N<sub>2</sub> and CO<sub>2</sub>/CH<sub>4</sub> selectivity than those of other MMMs by blending. In addition, Tien-Binh and Kaliaguine et al. [126] utilized PSP to graft UiO-66-NH<sub>2</sub> fillers with a PIM-1 monomer (i.e., trans-2-[3-(4-tert-Butylphenyl)-2-methyl-2-propenylidene] malononitrile (DCTB)), fabricating UiO-66 grafted PIM-1 MMMs. This approach significantly enhanced the CO<sub>2</sub> separation performance ~250 % and revealed the considerably intensified anti-aging effects in

comparison to MMMs prepared by conventional blending methods.

Recently, the attention to ionic liquid (IL) has been grown due to the non-volatility, favorable solubility for various molecules, and high sorption capacity for polar vapor/gas molecules such as H<sub>2</sub>O and CO<sub>2</sub> [128]. Yao and Dong et al. [129] adopted IL as a polymerizable grafting agent between UiO-66 and polyurethane oligomer to synthesis MMMs via PSP (Fig. 8c). The IL-modified UiO-66 formed covalent bonds with the isocyanate terminal groups of polyurethane oligomers. The filler loading of 50 wt% in the grafted MMMs enabled CO<sub>2</sub> permeance increased by 600 % and CO<sub>2</sub>/N<sub>2</sub> separation factor ~ 500 %.

#### 4.4.2. In-situ filler formation

**4.4.2.1. In solution.** One of the initial attempts to fabricating MMMs with in-situ filler formation involved the sol-gel synthesis of silica from precursors such as tetraethyl orthosilicate (TEOS) within a polymer solution [130]. Subsequently, Seoane and Coronas et al. [46] fabricated MOF-based MMMs by using the in-situ formation of MIL-68 (Al) fillers in a PSf solution. This approach entailed a novel synthesis method of MIL-68 (Al) in THF solvent, which also served as a solvent for PSf. The loading of MOF fillers in the resulting MMMs was estimated by the yield of MIL-68 (Al) particle under identical synthesis conditions. The in-situ formation of MIL-68 (Al) effectively mitigated particle agglomeration, achieving uniformly distributed fillers within the polymer at the filler loading of 8 wt%. The even distribution of fillers coupled with enhanced polymer/filler interactions led to enhanced H<sub>2</sub>/CH<sub>4</sub> and CO<sub>2</sub>/CH<sub>4</sub> selectivities with increased filler loading. In contrast, PSf/MIL-68 (Al) MMMs prepared by conventional blending methods exhibited severe particle agglomeration, resulting in a decrease in the gas selectivity

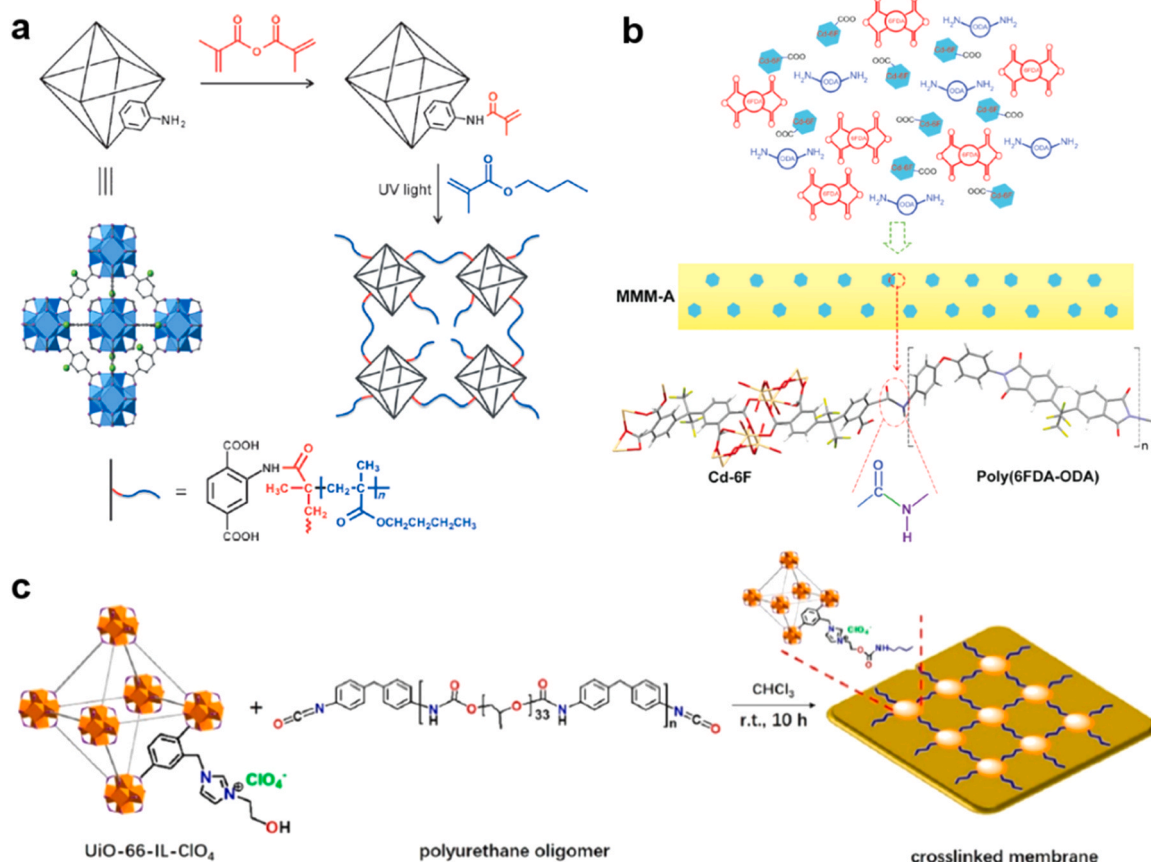


**Fig. 8.** (a) Post-synthetic modification of UiO-66-NH<sub>2</sub> with methacrylic anhydride and subsequent polymerization with butyl methacrylate by irradiation with UV light [127]. Copyright 2015, Wiley. (b) Diagram of designed interaction between Cd-6FDA and 6FDA-ODA in the grafted MMM [125]. Copyright 2014, American Chemical Society. (c) Chemically cross-linked membrane-based on UiO-66-IL-ClO<sub>4</sub> nanoparticles and the polyurethane oligomer [129]. Copyright 2017, American Chemical Society.

compared to that of the neat polymer membranes.

Differing from the Seoane and Coronas et al.'s work [46], which involved in-situ filler formation in the bulk polymer solution before film casting, recently, Matrimid®/UiO-66 MMMs were prepared by in-situ filler formation in the cast polymer solution (Fig. 9a) [131]. This direct fabrication strategy provided simultaneous synthesis of UiO-66 and film formation using a dope solution prepared through dissolving a polymer in the MOF precursor solution. It is important to note that the one-step approach significantly simplified the MMM preparation process, offering advantages for large-scale MMM production. The resulting MMMs showed improved interfacial interaction and filler distribution compared to those produced by conventional blending at the lower filler loading of ~ 2 wt%. Unfortunately, at the higher filler loading (i.e., ~ 11 wt%), severe particle agglomeration became inevitable, leading to diminished CO<sub>2</sub>/N<sub>2</sub> selectivity for MMMs prepared via in-situ filler formation beyond a 6 wt% filler loading, compared to MMMs prepared by blending.

He et al. [132] achieved high filler loading by in-situ growth ZIF-8 particles within PIM-1, inspired by the formation process of nodules in rhizobia for mutual symbiosis (Fig. 9b). By employing a CHCl<sub>3</sub>/water mix, they generated evenly distributed small ZIF-8 crystals (approximately 100 nm) within the highly permeable PIM-1 matrix, facilitating MOF loadings up to an impressive 67.2 wt%. Importantly, the interaction between the CN group in PIM-1 and the NH group in ZIF-8 ensured enhanced interfacial compatibility, effectively preventing the formation of nonselective flaws, even at high MOF concentrations. The resulting membrane exhibited remarkable CO<sub>2</sub> permeability (6338 barrer) while maintaining sufficient selectivity for energy-efficient carbon capture (the selectivity of CO<sub>2</sub>/N<sub>2</sub> is 24.4 and that of CO<sub>2</sub>/CH<sub>4</sub> is 18.8).

Li et al. [133] introduced a confined swelling coupled with

solvent-controlled crystallization method to produce defect-free MMMs enriched with MOF nanocrystals (Fig. 9c). Utilizing NH<sub>3</sub>·H<sub>2</sub>O and MeOH, they rapidly produce high-quality, large, and uniform ZIF-8 nanocrystals within an expanded PEO matrix in situ. This approach not only addresses the issue of pore blockage but also promotes the close arrangement of ZIF-8 nanocrystals. Consequently, the developed MMMs, enriched with ZIF-8 nanocrystals beyond a critical threshold, enhance the pathway for CO<sub>2</sub> mass transfer. Furthermore, the specific chelating interaction between ZIF-8 and PEO significantly enhanced CO<sub>2</sub>/N<sub>2</sub> selectivity. The optimized ZIF-8/PEO membrane demonstrates a CO<sub>2</sub> permeability of 2490 Barrer and a CO<sub>2</sub>/N<sub>2</sub> selectivity of 37, surpassing most PEO-based MMMs.

Jeong's group [134] has recently developed a novel in-situ MMM fabrication technique, termed phase-inversion in sync with MOF formation (PIMOF), effectively addressing commercialization challenges for MMMs. This method enabled the in-situ formation of ZIF-8 filler particles within the top polymer layers through the simultaneous phase-inversion of the polymer membrane and the nucleation and growth of ZIF-8 through counter-diffusion of zinc ions and 2-methylimidazole ligands in a dope solution and a quench bath, respectively (Fig. 9d). The PIMOF MMMs demonstrated exceptionally high performances in C<sub>3</sub>H<sub>6</sub>/C<sub>3</sub>H<sub>8</sub> separation with a C<sub>3</sub>H<sub>6</sub> permeance of 7.5 GPU and a separation factor of 107. The remarkable separation efficiency is likely due to the superior molecular sieving abilities of the ultra-small ZIF-8 nanofillers (less than 5 nm), combined with a high ZIF-8 content (more than 50 wt%) in the membrane skin layer. The PIMOF technique represents a significant advancement toward the commercialization of MMMs in gas separations.

#### 4.4.2.2. In solid membrane.

While in-situ filler formation in polymer

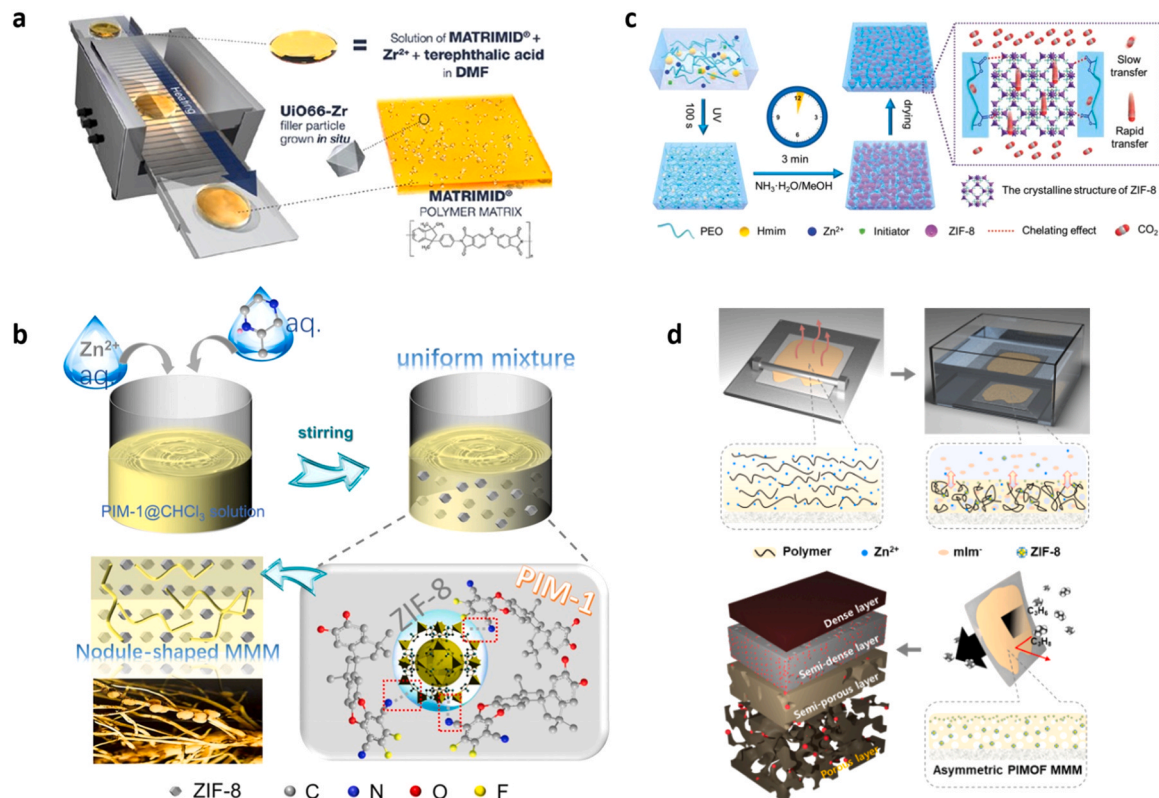


**Fig. 9.** (a) Schematic illustration of Matrimid®/UiO-66 MMMs fabrication via in-situ synthesis of UiO-66 in the polymer solution while simultaneous solvent evaporation by heating [131]. Copyright 2018, American Chemical Society. (b) Schematic illustrations of the preparation of ZIF-8/PIM-1 hybrid via the symbiosis-inspired in situ growth approach. Copyright 2021, National Academy of Sciences. (c) Schematic illustrations of the ZIF/PEO membrane preparation via the confined swelling coupled solvent-controlled crystallization (CSSC) strategy. Copyright 2023, Wiley. (d) Schematic illustration of the facile formation of an asymmetric PIMOF MMM by the phase-inversion in sync with MOF formation (PIMOF) process. Copyright 2023, Elsevier.

solutions has demonstrated potential by improving filler distribution, polymer/filler interfacial interaction, and scalability, its applications has been predominantly confined in low filler loadings (< 10 wt%) [131]. This limitation could be attributed to the polymer solution providing sufficient mobility for the in-situ formed crystals to rearrange themselves in order to minimize the surface energy, which leads to the agglomeration of in-situ formed crystals. Hence, as the concentration of in-situ formed fillers in the solution increases, the distance between in-situ formed fillers decreases, adversely affecting their distribution. In response to these, recent advancements have reported in-situ filler formations within solid polymer membranes, achieving more uniform filler distribution even at the higher filler loading (> 25 wt%) [135–137].

Ma and Tan et al. [135] proposed a new concept of MMM fabrication using in-situ filler formatting in a crosslinked polymer matrix. They mixed the precursors of PEO-based polymer and the precursors of ZIF-8 (i.e., zinc nitrate and 2-methylimidazole) without using solvents (Fig. 10a). Following polymerization, ZIF-8 fillers were in-situ formed within the crosslinked polymer upon the polymer swelling in water at room temperature. Despite achieving a uniform filler distribution compared to MMMs prepared by in-situ formation in a solution, the in-situ formed ZIF-8 fillers exhibited partial agglomeration. To avoid agglomerations potentially caused by the random distribution of ZIF-8 precursors, the polymer membrane containing ZIF-8 precursor underwent thermal treatment above the melting point of the polymer. This

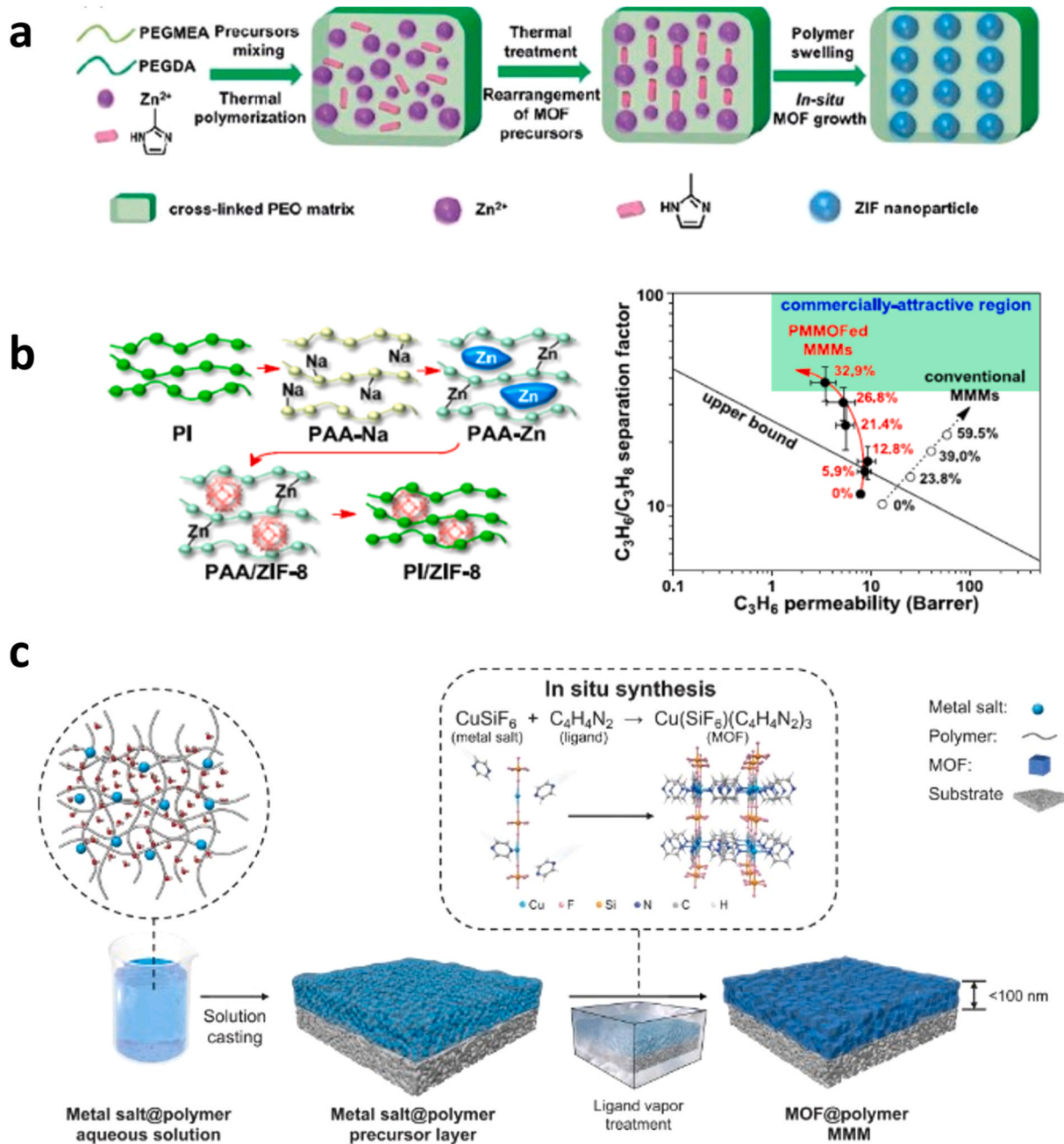


**Fig. 10.** (a) Schematic illustrations of the preparation of ZIF-based mixed matrix membranes using the in-situ growth approach. Copyright 2019, The Royal Society of Chemistry. (b) Schematic illustration of the in-situ ZIF-8 formation in the polymer free volume by PMMOF (left); propylene/propane separation performance of 6FDA-DAM/ZIF-8 MMMs prepared by the PMMOF and those of counterpart MMMs prepared by the blending method (right) [136]. Copyright 2019, American Chemical Society. (c) Schematic of the mixed-matrix membrane (MMM) fabricated by a solid-solvent processing (SSP) strategy. Copyright 2023, American Association for the Advancement of Science.

process led to the enhanced distribution of fillers with high compatibility with the polymer, achieving a ZIF-8 loading of up to 60 wt%. It is noted that the size of in-situ formed ZIF-8 increased with thermal treatment, growing from  $\sim 100$  nm to  $\sim 800$  nm in size. This tendency corresponded to an increase in the concentration of ZIF-8 precursors. The resulting MMM showed considerable enhancements in  $\text{CO}_2$  permeability.

Park and Jeong et al [136–138] reported the complete decoupling of in-situ filler formation in a polymer membrane from the polymer membrane processing for fabricating 6FDA-DAM/ZIF-8 MMMs. The decoupling potentially enabled more scalable MMM fabrications by directly upgrading a large-scale polymer hollow fiber membrane to a MMHFM with the general advantages of in-situ filler formation. The in-situ filler formation strategy named as polymer-modification-enabled in-situ metal-organic framework formation (PMMOF) comprises four steps: (1) polymer membrane hydrolysis and swelling, (2) ion-exchange, (3) ligand treatment, and (4) imidization (Fig. 10b). ZIF-8 nanocrystals were in-situ synthesized by the successively diffused ZIF-8 precursors within the polymer free volume enlarged by hydrolysis and swelling. The in-situ formed ZIF-8 in the polymer membrane showed homogeneous ZIF-8 distributions without any interfacial defects. By increasing Zn solution concentrations, ZIF-8 loading increased to  $\sim 33$  vol%, dramatically improving propylene/propane selectivity compared to that of counterparts prepared by conventional blending methods (Fig. 10b) [136]. Nevertheless, as shown in Fig. 10b, it was observed that an increase in filler contents resulted in decreased intrinsic polymer permeability, likely due to the reduction in polymer free volume filled by the in-situ formed fillers.

Chen et al [139] introduced a cutting-edge technique for producing ultra-thin MMMs heavily loaded with MOFs. By adopting a solid-solvent process, they achieved membrane thicknesses below 100 nanometers with  $\text{Cu}(\text{SiF}_6)(\text{pyz})_3$  loadings up to 80 vol%. This method involves the dissolution of metal salt  $\text{CuSiF}_6$  in a polymer (PEG or PVA) acting as a solid solvent and reacting with pyrazine vapor to produce thin and filler-rich MMMs (Fig. 10c). These membranes exhibit significantly improved  $\text{H}_2$  flow and selectivity, outperforming the capabilities of the best existing membranes, especially for efficient extraction of  $\text{H}_2$  from  $\text{CO}_2$ . The separation performance of  $\text{Cu}(\text{SiF}_6)(\text{pyz})_3@\text{PVA}$  MMM with an  $\text{H}_2$  permeance of 300 GPU and a  $\text{H}_2$  to  $\text{CO}_2$  selectivity of 30 positions alongside carbon molecular sieve (CMS) and MOF membranes.

## 5. Scale-up and commercialization of MMMs

The successful scale-up and commercialization of MMMs for gas separation are pivotal for transitioning from promising research outcomes to viable industrial applications. The integration of advanced materials and innovative fabrication techniques offers the potential to surpass the performance limitations of conventional polymer membranes, providing superior selectivity and permeability. However, achieving commercial success with MMMs requires addressing several critical factors, including the scalability of fabrication processes, economic viability, and meeting stringent performance benchmarks under real-world operational conditions.

Scalability in MMM fabrication is crucial to ensure that the membranes can be produced efficiently and cost-effectively at an industrial scale. This involves evaluating various fabrication methodologies to determine their ability to produce defect-free membranes with uniform filler dispersion and strong interfacial bonding. Additionally, the economic feasibility of these methods is assessed to identify the most cost-effective approaches for large-scale production. In parallel, it is essential to benchmark the performance of MMMs against established commercial standards. This includes not only achieving high gas permeance and selectivity but also ensuring that these properties are maintained under the specific operational conditions of intended applications. To pave the way for the commercialization of MMMs, we provide a comprehensive evaluation of current fabrication techniques, economic analyses, and

performance benchmarks. By addressing the challenges associated with scale-up and highlighting the most promising approaches, this work aims to guide future research and development efforts towards the successful industrial application of MMMs for gas separation.

### 5.1. Scalability evaluation of MMM processing

Scalability in MMM fabrication is pivotal for their transition to commercial applications. To assess the scalability of various MMM fabrication methodologies, key factors include: (1) the diversity of fabricable membrane modules, (2) the minimum defect-free thickness of selective layers, (3) adaptability in membrane material choices, (4) the ability to incorporate filler loadings while maintaining a defect-free microstructure, and (5) effectiveness in controlling potential defects such as polymer/filler interfacial voids, filler agglomeration, and pinhole formation in the skin layer. Utilizing these criteria, the scalability of different MMM fabrication technologies is systematically reviewed and summarized in Table 3.

Traditionally, the phase inversion method has been the cornerstone of large-scale MMM fabrications, particularly for MMHFs. Most MMHFs are produced using a dry jet-wet quench spinning process based on phase inversion principles. This technique is capable of producing asymmetric hollow fibers with ultra-thin selective layers (i.e., less than 1  $\mu\text{m}$ ) and thick porous support layers (i.e., greater than 100  $\mu\text{m}$ ) in a continuous, single-step process. However, despite the success of phase inversion in fabricating polymeric HFs, defect formation in thin MMM layers during the spinning process has emerged as a significant challenge [140]. Consequently, MMHFs made by phase inversion often require additional steps to seal these defects, a necessity attributed to the complex variables in the spinning process that affect the integrity and performance of the resultant membranes [140].

Conversely, there have been instances of successful large-scale MMM fabrications employing a straightforward dip-coating technique [141, 142]. This method involves separately preparing MMM skin layers and forming porous HF support layers through conventional spinning processes. Thin MMM skin layers are created on symmetrically porous HFs by simply immersing the HFs in an MMM solution, offering greater control over the fabrication process than phase inversion techniques for MMHFs. This approach notably improves issues related to pinhole formation and eliminates the need for additional polymer coating steps to seal defects. Additionally, the shear stress during dip-coating facilitates the parallel alignment of 2D GO particles within MMHFs, enhancing their structural properties [143]. Despite these advantages, the dip-coating method has not fully addressed the fundamental challenges associated with MMMs, such as interfacial adhesion and filler agglomeration [144].

In response to these challenges, fabricating MMMs via in-situ polymerization has emerged as a promising alternative. Specifically, PSP significantly improved the microstructures of MMMs and achieved remarkable filler loadings, potentially enhancing fabrication scalability. However, the specialized nature of polymer synthesis in PSP may limit material diversity, mainly to in-situ polymerizable monomers (e.g., those with vinyl functional groups) and MOF fillers with polymerizable functional groups. Moreover, IP represents another promising strategy for large-scale MMM fabrication, allowing commercial application in Thin-Film Composite (TFC) reverse osmosis (RO) membranes and nanofiltration (NF) membranes [145]. One of the most appealing aspects of IP lies in forming exceptionally thin selective polymer layers (i.e., less than 10 nm) due to the self-terminating reaction nature, significantly enhancing membrane performance. Nevertheless, challenges like filler agglomeration and pinhole formation remain significant barriers to the commercial development of MMHFs via IP. These issues underscore the need for ongoing research and development to refine in-situ polymerization techniques for a broader range of MMM applications.

Recently, the development of MMMs through in-situ filler formation has shown promising outcomes for future commercial applications.

**Table 3**  
Scalability evaluation of MMM processing.

MMM fabrication method	Module	Selective layer thickness	Material		Filler loading	Defect		Filler dispersion	Pinhole
			Polymer	Filler		Interfacial adhesion			
Solution processing	Solution-casting	PF, SW	< 10 μm	Most type	Most type	Moderate	Moderate	Moderate	Moderate
	Knife-casting	PF, SW	< 10 μm	Most type	Most type	Moderate	Moderate	Moderate	Moderate
	Spin-coating	PF	< 100 nm	Most type	Most type	Moderate	Moderate	Moderate	Moderate
	Dip-coating	PF, SW, HF	< 1 μm	Most type	Most type	Moderate	Moderate	Moderate	Moderate
Melt processing		PF, SW, HF	< 100 μm	Semicrystal	Thermally stable	Low	Good	Poor	Moderate
		PF, SW, HF	< 1 μm	Most type w/ high Mw	Water stable	Moderate	Moderate	Moderate	Poor
In-situ polymerization	In-situ crosslinking	PF, SW, HF	< 10 μm	In-situ polymerizable	Most type	High	Good	Good	Moderate
		PF, SW, HF	< 10 μm	In-situ polymerizable	MOF w/ functional groups	High	Excellent	Excellent	Moderate
	PSP	PF, SW, HF	< 10 nm	Polyamide	Water stable	Low	Good	Poor	Poor
		IP	< 10 nm						
In-situ filler formation	In solution	PF, SW, HF	< 10 μm	Most type	MOF	Low	Good	Poor	Moderate
	In solid membrane	PF, SW, HF	< 1 μm	Most type	MOF	High	Good	Excellent	Good

While in-situ filler growth within MMM dope solutions has led to filler agglomeration at high loadings, separating polymer membrane formation from in-situ filler synthesis presents a viable strategy to address the core challenges of MMMs. Although still in its early stages and requiring further refinement, this technique represents a promising pathway toward solving MMM scalability issues for commercial use, potentially enhancing MMM performance and applicability by optimizing filler distribution and integration within the membrane matrix.

## 5.2. Cost evaluation of MMM processing

An economical fabrication process is crucial for the commercial success of MMMs. An initial cost assessment for lab-scale MMM processing has been conducted as presented in [Table 4](#). While acknowledging that the costs associated with lab-scale MMM fabrication may differ from those at an industrial scale, this assessment can offer insights into the potential expenses involved in commercial MMM manufacturing across various processing technologies. The manufacturing costs of MMMs are categorized into several key areas: (1) material costs, (2) preparation costs of dope solutions, (3) equipment costs, (4) processing costs, (5) productivity, and (6) costs related to

waste recycling or disposal. It is important to identify a commercially viable form of MMM, and cost evaluations should reflect this consideration. As discussed in [Section 4.3](#), dual-layer MMMs are more cost-effective than single-layer MMMs due to the use of less expensive polymer materials for the porous support layer, conserving high-performance polymer and filler materials. Moreover, considering the superior surface-area-to-volume ratio, mixed-matrix hollow fiber membranes (MMHFs) are preferred over flat sheet MMMs for commercial applications, as detailed in [Section 3](#). Therefore, the economic analysis primarily focuses on dual-layer MMHFs, highlighting their potential for cost-effective scalability and commercial deployment. This approach underscores the importance of MMM fabrication techniques that meet both technical and performance criteria align with economic feasibility for widespread industrial application.

Dual-layer MMHFs are predominantly manufactured using the conventional phase-inversion-induced dry jet-wet quench spinning process, which enhances productivity and potentially lowers the cost per membrane unit. However, material costs tend to be higher due to the high concentration of polymers and fillers in the mixed-matrix dope solution (i.e., > 20 wt% for phase inversion vs. < 5 wt% for dip-coating). The spinning systems for dual-layer MMHFs including

**Table 4**  
Cost evaluation of lab-scale MMM processing.

MMM fabrication method	Material and preparation			aEquipment	Processing	Productivity	Waste
	Polymer	Filler	Solution				
Solution processing	Solution-casting	Cheap	Blending w/ solvent	< 1k USD	Cheap: solvent evaporation	Low	Moderate
		Moderate			< 2k USD	Cheap: solvent evaporation	Low
		Moderate			< 10k USD	Moderate: centrifugation	Moderate
		Cheap			< 6k USD	Cheap: solvent evaporation	High
Melt processing	Dip-coating	Cheap	w/o solvent	< 3k USD	Expensive: heating	High	Moderate
		Expensive			< 50k USD	Expensive: large volume of non-solvent	High
Phase inversion	In-situ crosslinking	Monomers	Blending w/ solvent	< 1k USD	Moderate: polymerization	Moderate	Low
		Monomers			< 1k USD	Moderate: polymerization	Low
In-situ polymerization	PSP	Expensive	Blending w/ solvent	< 1k USD	Moderate: sequential immersing	Moderate	Low
		Monomers			< 1k USD	Moderate: filler synthesis	Low
In-situ filler formation	In solution	Moderate	Precursors	Blending not required	< 1k USD	Moderate: sequential immersing	Moderate
		Cheap					Low
	In solid membrane	Cheap	Precursors				

<sup>a</sup> Roughly estimated minimum costs.

components like three syringe pumps, a dual-layer spinneret, a quench bath, and a take-up drum, incur higher expenses compared to systems used for single-layer polymer HFM. Additionally, the extensive use of non-solvent in the coagulation bath during spinning escalates energy use and costs, including those for temperature control of the coagulation bath and disposal of non-solvent.

Melt processing presents a less costly alternative for spinning equipment compared to phase inversion, as it eliminates the need for solvents and non-solvents. However, the high temperatures required for polymer melting and membrane extrusion could increase energy expenditures. Conversely, while most solution processing-based MMM fabrications are batch processes unsuitable for MMHFM production, the dip-coating method emerges as an economically viable option for commercial MMM production due to its low material and capital costs, straightforward operation, and high productivity.

In-situ techniques leverage the benefits of dip-coating for dual-layer MMHFM by applying a thin selective layer onto a porous polymeric support, additionally minimizing waste through in-situ polymerization or filler crystallization. Although certain in-situ methods may require complex and costly material synthesis and modifications, MMM fabrication via in-situ techniques generally avoids the need for specialized, expensive equipment and processes. Consequently, in-situ methods appear more cost-effective than traditional phase inversion-based MMM fabrications, offering both high scalability and economic efficiency as compelling advantages for future commercial applications.

### 5.3. Commercially available MMM separation performance criteria

While numerous studies have confirmed that the separation performances of MMMs can exceed beyond the established upper bound curves by incorporating appropriate fillers, merely surpassing these benchmarks does not guarantee their commercial success. For MMMs to be commercially viable, any enhancement in separation performance must meet the specific minimum requirements of their intended applications[146]. In essence, if an MMM's selectivity greatly surpasses the upper bound curve but its permeance (or permeability) falls short of the benchmarks set by commercially available technologies for the same separation task, then its superior performance does not translate to commercial attractiveness. This assessment holds true if the roles of selectivity and permeance are reversed. Furthermore, it is crucial to recognize that MMMs must not only meet the separation performance requirements but also sustain these commercial benchmarks under the operational conditions they will face in real-world applications. To facilitate a clearer understanding of those requirements, we have compiled a summary of membrane-based gas separation performance

criteria, along with their operational conditions, for several key commercial applications in Table 5.

In addition to separation performance, the long lifespan of MMMs in industrial applications is a critical factor influencing their commercial viability. Several factors affect the longevity of MMMs, including the specific application, operational conditions, and the type of materials used. The chemical and thermal stability of both the polymer matrix and the filler material are crucial in determining the membrane's durability. Exposure to harsh operating environments, such as high temperatures, pressure, and aggressive chemicals, can deteriorate separation performance. The lifespan of current polymer membranes used in the gas separation industry typically ranges from 3 to 5 years[147]. Despite the limitation for commercialized MMMs, MMMs often exhibit greater long-term stability than polymer membranes[148]. This is because robust inorganic fillers in MMMs, with good adhesion, compensate for the reduction of excessive free volume in the polymer due to physical aging and provide resistance to plasticization for condensable gases at high pressure. Therefore, achieving good interfacial adhesion of fillers with the polymer matrix through appropriate materials and processing can increase the lifespan of MMMs in industrial applications.

## 6. Outlook

While polymer membranes are already commercially employed for various gas separations, the potential market for gas separation could significantly expand with the development of commercial MMMs that offer superior gas separation performance to current polymer membranes. For instance, in the domain of C3 (propylene/propane) separation, substituting distillation systems with one of the top-performing polymer membranes, 6FDA-TrMPD (which boasts a C<sub>3</sub>H<sub>6</sub> permeance of 7.5 GPU and a C<sub>3</sub>H<sub>6</sub>/C<sub>3</sub>H<sub>8</sub> selectivity of 11), results in an approximate 25 % increase in the C3 separation operating costs due to the high expenses associated with membrane maintenance[162]. This scenario highlights that polymer membranes alone may not be economically viable for commercial C3 separation. A distillation-membrane hybrid system presents a potential alternative, modestly reducing operating costs from \$9.7 million to \$8.9 million USD/year[162]. However, if the C3 separation performance of membranes be elevated to C<sub>3</sub>H<sub>6</sub> permeance of 21 GPU and C<sub>3</sub>H<sub>6</sub>/C<sub>3</sub>H<sub>8</sub> selectivity of 42—figures slightly above those reported for MMHFM—the economic benefits of membrane-based C3 separation would exceed those of distillation systems, halving the operation costs[162]. This improvement underscores the transformative potential of commercial MMMs in reshaping the gas separation market. Accordingly, pursuing innovative MMM fabrication strategies from an engineering standpoint becomes crucial. Addressing

**Table 5**  
Membrane-based gas separation performance criteria for commercial applications.

Application	Market size (USD/year)	Gas pair	General operation condition	Desired gas permeance (or permeability)	Desired gas selectivity	Ref.
Air-dehumidification	900 million	H <sub>2</sub> O/N <sub>2</sub>	22 °C (indoor) or 30 °C (outdoor) 60 ~ 80 % RH	> 11900 GPU	> 1500	[149,150]
Pre-combustion CO <sub>2</sub> capture	1.8 billion	H <sub>2</sub> /CO <sub>2</sub>	250 ~ 400 °C Total feed pressure of 20 bar	200 ~ 1000 GPU	> 10	[151,152]
Hydrogen recovery from ammonia purge gas	200 million	H <sub>2</sub> /N <sub>2</sub>	60 % H <sub>2</sub> , 20 % N <sub>2</sub> Transmembrane pressure of 40 bar	> 1000 GPU	> 290	[1,153,154]
Hydrogen production by gas steam reforming	120 billion	H <sub>2</sub> /CH <sub>4</sub>	40 °C Transmembrane pressure of 4 bar	> 85 GPU	> 37	[155]
Post-combustion CO <sub>2</sub> capture	700 million	CO <sub>2</sub> /N <sub>2</sub>	Low CO <sub>2</sub> partial pressure 5 % CO <sub>2</sub>	1000 ~ 5000 GPU	30 ~ 50	[52,151,156]
Natural gas upgrading	300 million	CO <sub>2</sub> /CH <sub>4</sub>	10 % CO <sub>2</sub> , 50 °C Total feed pressure of 70 bar	> 100 GPU	20 ~ 35	[49,157]
Air separation	800 million	O <sub>2</sub> /N <sub>2</sub>	21 % O <sub>2</sub> , 79 % N <sub>2</sub> Total feed pressure of ~ 10 bar	> 0.8 Barrer	> 8	[34,157-159]
Olefin production from steam cracking	37 billion	C <sub>2</sub> H <sub>4</sub> /C <sub>2</sub> H <sub>6</sub>	Total feed pressure of > 6 bar	> 30 GPU	> 30	[160]
		C <sub>3</sub> H <sub>6</sub> /C <sub>3</sub> H <sub>8</sub>		> 1 Barrer	> 35	[161]

and surmounting the challenges that currently hinder the commercialization of MMMs is essential to unlocking their full market potential, offering more efficient and cost-effective solutions for gas separation that could replace or complement existing technologies.

The integration of various MMM fabrication strategies is anticipated to yield synergistic effects that accelerate commercialization. Among the array of fabrication approaches, MMMs created through in-situ filler formation stand out for their significantly enhanced scalability and reasonable manufacturing costs compared to traditional methods. This technique necessitates the initial formation of a thin polymer layer, crucial to the process's success. Despite challenges such as pinhole formation and filler agglomeration, this method remains appealing for producing defect-free ultra-thin polymer membranes [119,120]. Therefore, leveraging the in-situ filler formation approach, a TFC membrane produced via the IP technique could be effectively transformed into a TFN, facilitating the fabrication of large-scale MMMs with selective layers just a few nanometers thick. This advancement signifies a substantial leap forward in the field of membrane fabrication technology, potentially realizing the promise of MMMs that combine the benefits of enhanced separation performance and economic viability.

Computational studies have become indispensable tools in accelerating the development of commercially viable MMMs for gas separation, and their importance is expected to grow in the future. Despite the extensive variety of polymer and molecular sieve materials, only a select few have been explored for their potential in MMMs for gas separations. For example, as of 2017, approximately 70,000 MOFs were registered in the Cambridge Structural Database, showcasing the vast potential for materials exploration [163]. High-throughput computational simulations are particularly notable for their ability to screen materials for MMMs at speeds unattainable by experimental methodologies. Qiao et al [164] demonstrated the efficiency of such computational approaches by screening over 6000 MOFs for gas separations, identifying the most suitable MOF structures for fifteen gas pairs based on predicted gas transport results. Similarly, Jiang et al. [165] assessed the three-component (CO<sub>2</sub>/N<sub>2</sub>/CH<sub>4</sub>) gas separation performance of 4800 MOFs through simulations that combined Monte Carlo (for gas adsorption) and molecular dynamics (for gas diffusion) techniques. These examples emphasize the critical role of developing advanced gas transport simulation models to enable more accurate and reliable predictions of gas separation performances in MMMs. Such advancements in computational methods will not only streamline the selection of materials for MMMs but also significantly contribute to the design of membranes with optimized microstructures, thereby optimized separation properties, paving the way for their commercial application in gas separation technologies.

Efforts to more closely align predictions with experimental outcomes have led to the exploration of mathematical models that incorporate the morphological characteristics of MMMs, including non-ideal factors such as pore blockage by fillers, polymer rigidification, filler agglomeration, interfacial voids, among others [8,22,166]. Traditionally, the Maxwell model has been widely used to predict the gas separation performance of MMMs. However, its applicability is limited to ideal MMMs with relatively low filler loadings and spherical fillers due to its oversimplification of filler morphologies and the interactions between components. To address these limitations, various advanced modeling approaches have been developed, including resistance-based models [167], simulation-based rigorous models [168], and effective-medium theory-based models [169]. These sophisticated simulation models are being actively refined to enhance control microstructures and facilitate rational designs for commercial MMMs. The development of these models represents a significant advancement in the field, enabling more precise design and optimization of MMMs for enhanced performance.

## 7. Summary

MMMs have attracted considerable attention over the past decades,

establishing themselves as a significant area of research due to their unique advantages. These advantages encompass the reproducibility, flexibility, and low cost associated with polymeric membranes, combined with the superior gas separation performance characteristic of inorganic fillers. This review covers the development of MMMs for gas separation, highlighting their potential and engineering challenges for commercialization. The effectiveness of MMMs is influenced not only by the choice of materials but also by the fabrication methods employed. The spectrum ranges from traditional solution processing to innovative in-situ formation techniques, evaluating their ability to enhance adhesion between organic and inorganic phases and to optimize filler dispersion from an engineering perspective. Achieving a continuous defect-free robust selective layer with minimal thickness and maximal filler loading is crucial for attaining optimal gas separation performance. While the solution process is simple and direct, it is predominantly used for producing flat sheet MMMs, which suffer from relatively low productivity. MMMs fabricated via melt processing exhibit excellent interfacial adhesion but at the cost of increased energy consumption. The in-situ formation process, on the other hand, offers promising prospects for the interfacial morphology and integrity of MMMs, albeit with limitations related to material compatibility. Among various configurations, mixed-matrix hollow fiber membranes (MMHFs) stand out as particularly attractive to the industry, thanks to their high packing density and low processing costs compared to other modules. Commercially, MMHFs are typically manufactured using a dry jet-wet spinning strategy, often supplemented by a dip-coating step to enhance membrane performance.

In summary, the scalability and cost-effectiveness of each fabrication strategy are critical factors for aligning with industry demands. To garner commercial interest, strategies must aim for a reduction in fabrication costs and an enhancement in the scalability of production. Taking these factors into account, dual-layer HFMMMs fabricated via in-situ methods are identified as the most promising candidates for future market dominance. Furthermore, the ambition for MMMs extends beyond merely overcoming the traditional trade-off between permeability and selectivity. Setting specific gas separation performance criteria related to practical applications is essential. While most MMM research has focused on CO<sub>2</sub> capture, the development of MMMs for other valuable separation systems, such as ethylene/ethane and propylene/propane, is progressing. The anticipation for the next generation of MMMs lies in their potential to facilitate practical, energy-efficient gas separations, marking a significant advancement in membrane technology.

## CRediT authorship contribution statement

**Yinying Hua:** Writing – review & editing, Writing – original draft, Investigation. **Sunghwan Park:** Writing – review & editing, Writing – original draft, Supervision. **Hae-Kwon Jeong:** Writing – review & editing, Supervision, Conceptualization.

## Declaration of Competing Interest

The authors declare that they have no known competing financial interests or personal relationships that could have appeared to influence the work reported in this paper.

## Data availability

Data will be made available on request.

## Acknowledgements

S.P. acknowledges partial financial support from the Ministry of Trade, Industry and Energy (MOTIE) (No. RS-2023-00266205) and Songwol Towel Co., Ltd. H.-K.J is grateful for the financial support from

the National Science Foundation (CBET-1929596) and the Korea Evaluation Institute of Industrial Technology (KEIT) funded by the Ministry of Trade, Industry & Energy (MOTIE, Korea) (Project: 20018346).

## References

- R. Spillman, Chapter 13 Economics of gas separation membrane processes, in: R. D. Noble, S.A. Stern (Eds.), *Membrane Science and Technology*, Elsevier, Amsterdam, 1995, pp. 589–667.
- L.M. Robeson, The upper bound revisited, *J. Membr. Sci.* 320 (1-2) (2008) 390–400, <https://doi.org/10.1016/j.memsci.2008.04.030>.
- B.D. Freeman, Basis of permeability/selectivity tradeoff relations in polymeric gas separation membranes, *Macromolecules* 32 (2) (1999) 375–380, <https://doi.org/10.1021/ma9814548>.
- K. Vanherck, G. Koeckelberghs, I.F.J. Vankelecom, Crosslinking polyimides for membrane applications: a review, *Prog. Polym. Sci.* 38 (6) (2013) 874–896, <https://doi.org/10.1016/j.progpolymsci.2012.11.001>.
- M.A. Carreton, S.G. Li, J.L. Falconer, R.D. Noble, Alumina-supported SAPO-34 membranes for CO<sub>2</sub>/CH<sub>4</sub> separation, *J. Am. Chem. Soc.* 130 (16) (2008) 5412–5413, <https://doi.org/10.1021/ja801294f>.
- M.Y. Jeon, D. Kim, P. Kumar, P.S. Lee, N. Rangnekar, P. Bai, M. Shete, B. Elyassi, H.S. Lee, K. Narasimharao, S.N. Basahel, S. Al-Thabaiti, W.Q. Xu, H.J. Cho, E. O. Fetisov, R. Thyagarajan, R.F. DeJaco, W. Fan, K.A. Mkoyan, J.I. Siepmann, M. Tsapatsis, Ultra-selective high-flux membranes from directly synthesized zeolite nanosheets, *Nature* 543 (7647) (2017) 690–694, <https://doi.org/10.1038/nature21421>.
- W.J. Koros, R. Mahajan, Pushing the limits on possibilities for large scale gas separation: which strategies? *J. Membr. Sci.* 175 (2) (2000) 181–196, [https://doi.org/10.1016/S0376-7388\(00\)00418-X](https://doi.org/10.1016/S0376-7388(00)00418-X).
- H. Vinh-Thang, S. Kaliaguine, A comprehensive computational strategy for fitting experimental permeation data of mixed matrix membranes, *J. Membr. Sci.* 452 (2014) 271–276, <https://doi.org/10.1016/j.memsci.2013.10.020>.
- M.W. Anjum, B. Bueken, D. De Vos, I.F.J. Vankelecom, MIL-125(Ti) based mixed matrix membranes for CO<sub>2</sub> separation from CH<sub>4</sub> and N<sub>2</sub>, *J. Membr. Sci.* 502 (2016) 21–28, <https://doi.org/10.1016/j.memsci.2015.12.022>.
- G. Dong, H. Li, V. Chen, Challenges and opportunities for mixed-matrix membranes for gas separation, *J. Mater. Chem. A* 1 (15) (2013) 4610–4630, <https://doi.org/10.1039/C3TA00927K>.
- X. Guo, Z. Qiao, D. Liu, C. Zhong, Mixed-matrix membranes for CO<sub>2</sub> separation: role of the third component, *J. Mater. Chem. A* 7 (43) (2019) 24738–24759, <https://doi.org/10.1039/C9TA09012F>.
- D. Bastani, N. Esmaeili, M. Asadollahi, Polymeric mixed matrix membranes containing zeolites as a filler for gas separation applications: a review, *J. Ind. Eng. Chem.* 19 (2) (2013) 375–393, <https://doi.org/10.1016/j.jiec.2012.09.019>.
- L. Gao, C. Li, W. Huang, S. Mei, H. Lin, Q. Ou, Y. Zhang, J. Guo, F. Zhang, S. Xu, H. Zhang, MXene/polymer membranes: synthesis, properties, and emerging applications, *Chem. Mater.* 32 (5) (2020) 1703–1747, <https://doi.org/10.1021/acs.chemmater.9b04408>.
- A.R. Kamble, C.M. Patel, Z.V.P. Murthy, A review on the recent advances in mixed matrix membranes for gas separation processes, 111062-11079, *Renew. Sustain. Energy Rev.* 145 (2021), <https://doi.org/10.1016/j.rser.2021.111062>.
- W. Guan, Y. Dai, C. Dong, X. Yang, Y. Xi, Zeolite imidazolate framework (ZIF)-based mixed matrix membranes for CO<sub>2</sub> separation: a review, 48968–48980, *J. Appl. Polym. Sci.* 137 (33) (2020), <https://doi.org/10.1002/app.48968>.
- R. Lin, B. Villacorta Hernandez, L. Ge, Z. Zhu, Metal organic framework based mixed matrix membranes: an overview on filler/polymer interfaces, *J. Mater. Chem. A* 6 (2) (2018) 293–312, <https://doi.org/10.1039/C7TA07294E>.
- S. Yu, C. Li, S. Zhao, M. Chai, J. Hou, R. Lin, Recent advances in the interfacial engineering of MOF-based mixed matrix membranes for gas separation, *Nanoscale* 16 (16) (2024) 7716–7733, <https://doi.org/10.1039/D4NR00096J>.
- S.H. Goh, H.S. Lau, W.F. Yong, Metal-organic frameworks (MOFs)-based mixed matrix membranes (MMMs) for gas separation: a review on advanced materials in harsh environmental applications, 2107536–2107559, *Small* 18 (20) (2022), <https://doi.org/10.1002/smll.202107536>.
- Z. Qin, Y. Ma, J. Wei, H. Guo, B. Wang, J. Deng, C. Yi, N. Li, S. Yi, Y. Deng, W. Du, J. Shen, W. Jiang, L. Yao, L. Yang, Z. Dai, Recent progress in ternary mixed matrix membranes for CO<sub>2</sub> separation, *GEE* 9 (5) (2024) 831–858, <https://doi.org/10.1016/j.gee.2023.04.008>.
- M. Mohsenpour Tehrani, E. Chehrezi, Metal–Organic-frameworks based mixed-matrix membranes for CO<sub>2</sub> separation: An applicable-conceptual approach, *ACS Appl. Mater. Interfaces* 16 (26) (2024) 32906–32929, <https://doi.org/10.1021/acsami.4c06914>.
- A.S. Reddy, P. Sharda, S.P. Nehra, A. Sharma, Advanced strategies in MOF-based mixed matrix membranes for propylene/propane separation: a critical review, 215435–215448, *Coord. Chem. Rev.* 498 (2024), <https://doi.org/10.1016/j.ccr.2023.215435>.
- H. Vinh-Thang, S. Kaliaguine, Predictive models for mixed-matrix membrane performance: a review, *Chem. Rev.* 113 (7) (2013) 4980–5028, <https://doi.org/10.1021/cr3003888>.
- M. Kim, W. Choi, C.H. Lee, D.W. Kim, 2D MOFs and zeolites for composite membrane and gas separation applications: A brief review, *ACS Mater. Au* 4 (2) (2024) 148–161, <https://doi.org/10.1021/acsmaterialsau.3c00072>.
- S. Kulprathipanja, Mixed matrix membrane development, *Membr. Technol.* 2002 (4) (2002) 9–12, [https://doi.org/10.1016/S0958-2118\(02\)80132-X](https://doi.org/10.1016/S0958-2118(02)80132-X).
- J.K. Neubert, Das Verhalten von Kautschuk zu Kohlensäure, 136–136, *Z. Chem. Ind. Kolloide* 11 (3) (1912), <https://doi.org/10.1007/BF01465813>.
- G.F. Christen, A.; Faure, A., Membrane Hétérogène Pour le Fractionnement de Mélanges Fluides, et Son Emploi, France, 1971.
- D.R. Kemp, D.R. Paul, Gas sorption in polymer membranes containing adsorptive fillers, *J. Polym. Sci., Polym. Phys. Ed.* 12 (3) (1974) 485–500, <https://doi.org/10.1002/pol.1974.180120304>.
- S.K.W.N.N. Li, Separation of fluids by means of mixed matrix membranes, United States, 1988.
- L.M. Robeson, Correlation of separation factor versus permeability for polymeric membranes, *J. Membr. Sci.* 62 (2) (1991) 165–185, [https://doi.org/10.1016/0376-7388\(91\)80060-J](https://doi.org/10.1016/0376-7388(91)80060-J).
- L.M. Robeson, The upper bound revisited, *J. Membr. Sci.* 320 (1) (2008) 390–400, <https://doi.org/10.1016/j.memsci.2008.04.030>.
- M. Jia, K.-V. Peinemann, R.-D. Behling, Molecular sieving effect of the zeolite-filled silicone rubber membranes in gas permeation, *J. Membr. Sci.* 57 (2) (1991) 289–292, [https://doi.org/10.1016/S0376-7388\(00\)80684-5](https://doi.org/10.1016/S0376-7388(00)80684-5).
- J.-M. Duval, A.J.B. Kemperman, B. Folkers, M.H.V. Mulder, G. Desgrandchamps, C.A. Smolders, Preparation of zeolite filled glassy polymer membranes, *J. Appl. Polym. Sci.* 54 (4) (1994) 409–418, <https://doi.org/10.1002/app.1994.070540401>.
- R.H.B. Bouma, A. Checchetti, G. Chidichimo, E. Drioli, Permeation through a heterogeneous membrane: the effect of the dispersed phase, *J. Membr. Sci.* 128 (2) (1997) 141–149, [https://doi.org/10.1016/S0376-7388\(96\)00303-1](https://doi.org/10.1016/S0376-7388(96)00303-1).
- R. Mahajan, W.J. Koros, Factors controlling successful formation of mixed-matrix gas separation materials, *Ind. Eng. Chem. Res* 39 (8) (2000) 2692–2696, <https://doi.org/10.1021/ie990799r>.
- H.C.F. David Richard Corbin, Mark Brandon Shiflett, Mixed matrix nanoporous carbon membranes, United States, 2001.
- S.S.K. Okan Max Ekiner, Process for making hollow fiber mixed matrix membranes, United States, 2003.
- H. Yehia, T.J. Pisklak, J. Ferraris, K. Balkus, I.H. Musselman, Methane facilitated transport using copper(II) biphenyl dicarboxylatetriethylenediamine/poly(3-acetoxyethylthiophene) mixed matrix membranes, *Polym. Prepr.* 45 (2004) 35–36.
- H.-K. Jeong, W. Krych, H. Ramanan, S. Nair, E. Marand, M. Tsapatsis, Fabrication of polymer/selective-flake nanocomposite membranes and their use in gas separation, *Chem. Mater.* 16 (20) (2004) 3838–3845, <https://doi.org/10.1021/cm049154u>.
- S. Takahashi, D.R. Paul, Gas permeation in poly(ether imide) nanocomposite membranes based on surface-treated silica. Part 1: without chemical coupling to matrix, *Polymer* 47 (21) (2006) 7519–7534, <https://doi.org/10.1016/j.polymer.2006.08.029>.
- S. Shu, W.J. Husain, Koros, Formation of nanostructured zeolite particle surfaces via a halide/grignard Route, *Chem. Mater.* 19 (16) (2007) 4000–4006, <https://doi.org/10.1021/cm070969n>.
- M.J.C. Ordoñez, K.J. Balkus, J.P. Ferraris, I.H. Musselman, Molecular sieving realized with ZIF-8/Matrimid® mixed-matrix membranes, *J. Membr. Sci.* 361 (1) (2010) 28–37, <https://doi.org/10.1016/j.memsci.2010.06.017>.
- T.-H. Bae, J.S. Lee, W. Qiu, W.J. Koros, C.W. Jones, S. Nair, A high-performance gas-separation membrane containing submicrometer-sized metal-organic framework crystals, *Angew. Chem. Int. Ed.* 49 (51) (2010) 9863–9866, <https://doi.org/10.1002/anie.201006141>.
- K.S. Park, Z. Ni, A.P. Côté, J.Y. Choi, R. Huang, F.J. Uribe-Romo, H.K. Chae, M. O'Keefe, O.M. Yaghi, Exceptional chemical and thermal stability of zeolitic imidazolate frameworks, *PNAS* 103 (27) (2006) 10186–10191, <https://doi.org/10.1073/pnas.0602439103>.
- J. Ahn, W.-J. Chung, I. Pinna, J. Song, N. Du, G.P. Robertson, M.D. Guiver, Gas transport behavior of mixed-matrix membranes composed of silica nanoparticles in a polymer of intrinsic microporosity (PIM-1), *J. Membr. Sci.* 346 (2) (2010) 280–287, <https://doi.org/10.1016/j.memsci.2009.09.047>.
- X. Yu, Z. Wang, J. Zhao, F. Yuan, S. Li, J. Wang, S. Wang, An effective method to improve the performance of fixed carrier membrane via incorporation of CO<sub>2</sub>-selective adsorptive silica nanoparticles, *Chin. J. Chem. Eng.* 19 (5) (2011) 821–832, [https://doi.org/10.1016/S1004-9541\(11\)60062-1](https://doi.org/10.1016/S1004-9541(11)60062-1).
- B. Seoane, V. Sebastián, C. Téllez, J. Coronas, Crystallization in THF: the possibility of one-pot synthesis of mixed matrix membranes containing MOF MIL-68(Al), *CrystEngComm* 15 (45) (2013) 9483–9490, <https://doi.org/10.1039/C3CE40847G>.
- X. Li, Y. Cheng, H. Zhang, S. Wang, Z. Jiang, R. Guo, H. Wu, Efficient CO<sub>2</sub> capture by functionalized graphene oxide nanosheets as fillers to fabricate multi-permselective mixed matrix membranes, *ACS Appl. Mater. Interfaces* 7 (9) (2015) 5528–5537, <https://doi.org/10.1021/acsami.5b00106>.
- V. Mari, M. Bhagiyalakshmi, Y. Alqaheem, A. Alomair, A. Pérez, M. Rana, Recent progress of Fillers in Mixed Matrix Membranes for CO<sub>2</sub> separation: a review, *Sep Purif. Technol.* 188 (2017) 431–450, <https://doi.org/10.1016/j.seppur.2017.07.051>.
- M. Galizia, W.S. Chi, Z.P. Smith, T.C. Merkel, R.W. Baker, B.D. Freeman, 50th anniversary perspective: polymers and mixed matrix membranes for gas and vapor separation: A review and prospective opportunities, *Macromolecules* 50 (20) (2017) 7809–7843, <https://doi.org/10.1021/acs.macromol.7b01718>.
- W. Li, F. Pan, Y. Song, M. Wang, H. Wang, S. Walker, H. Wu, Z. Jiang, Construction of molecule-selective mixed matrix membranes with confined mass transfer structure, *Chin. J. Chem. Eng.* 25 (11) (2017) 1563–1580, <https://doi.org/10.1016/j.cjche.2017.04.015>.

[51] M.R.A. Hamid, H.-K. Jeong, Recent advances on mixed-matrix membranes for gas separation: opportunities and engineering challenges, *Korean J. Chem. Eng.* 35 (8) (2018) 1577–1600, <https://doi.org/10.1007/s11814-018-0081-1>.

[52] H.B. Park, J. Kamcev, L.M. Robeson, M. Elimelech, B.D. Freeman, Maximizing the right stuff: the trade-off between membrane permeability and selectivity, *Science* 356 (2017) eaab0530, <https://doi.org/10.1126/science.aab0530>.

[53] A. Ebadi Amooghin, S. Mashhadikhan, H. Sanaeepur, A. Moghadassi, T. Matsuura, S. Ramakrishna, Substantial breakthroughs on function-led design of advanced materials used in mixed matrix membranes (MMMs): a new horizon for efficient CO<sub>2</sub> separation, *Prog. Mater. Sci.* 102 (2019) 222–295, <https://doi.org/10.1016/j.jpmatsci.2018.11.002>.

[54] Z. Kang, Y. Peng, Y. Qian, D. Yuan, M.A. Addicoat, T. Heine, Z. Hu, L. Tee, Z. Guo, D. Zhao, Mixed matrix membranes (MMMs) comprising exfoliated 2D covalent organic frameworks (COFs) for efficient CO<sub>2</sub> separation, *Chem. Mater.* 28 (5) (2016) 1277–1285, <https://doi.org/10.1021/acs.chemmater.5b02902>.

[55] T. Xu, P.P. Zhang, F.C. Cui, J.T. Li, L. Kan, B.B. Tang, X.Q. Zou, Y.L. Liu, G.S. Zhu, Fine-tuned ultra-microporous metal-organic framework in mixed-matrix membrane: pore-tailoring optimization for C<sub>2</sub>H<sub>2</sub>/C<sub>2</sub>H<sub>4</sub> separation, 2204553–2204562, *Adv. Mater.* 35 (13) (2023), <https://doi.org/10.1002/adma.202204553>.

[56] S.J. Datta, A. Mayoral, N.M.S. Bettahalli, P.M. Bhatt, M. Karunakaran, I.D. Carja, D. Fan, P.G.M. Mileo, R. Semino, G. Maurin, O. Terasaki, M. Eddaoudi, Rational design of mixed-matrix metal-organic framework membranes for molecular separations, *Science* 376 (6597) (2022) 1080–1087, <https://doi.org/10.1126/science.abe0192>.

[57] J. Wu, C.Z. Liang, A. Naderi, T.S. Chung, Tunable supramolecular cavities molecularly homogenized in polymer membranes for ultraefficient precombustion CO<sub>2</sub> capture, 2105156–2105164, *Adv. Mater.* 34 (3) (2022), <https://doi.org/10.1002/adma.202105156>.

[58] X.Y. Tan, S. Robijns, R. Thuer, Q.L. Ke, N. De Witte, A. Lamaire, Y. Li, I. Aslam, D. Van Havere, T. Donckels, T. Van Assche, V. Van Speybroeck, M. Dusselier, I. Vankelecom, Truly combining the advantages of polymeric and zeolite membranes for gas separations, *Science* 378 (6625) (2022) 1189–1194, <https://doi.org/10.1126/science.adf1411>.

[59] L.Q. Hu, K.W. Chen, W.I. Lee, K. Kisslinger, C. Rumsey, S.H. Fan, V.T. Bui, N. Esmaeili, T. Tran, Y.F. Ding, M. Trebbin, C.Y. Nam, M.T. Swihart, H.Q. Lin, Palladium-percolated networks enabled by low loadings of branched nanorods for enhanced H<sub>2</sub> separations, 2301007–2301014, *Adv. Mater.* 35 (26) (2023), <https://doi.org/10.1002/adma.202301007>.

[60] M. Mubashir, Y.Y. Fong, C.T. Leng, L.K. Keong, Issues and current trends of hollow-fiber mixed-matrix membranes for CO<sub>2</sub> separation from N<sub>2</sub> and CH<sub>4</sub>, *Chem. Eng. Technol.* 41 (2) (2018) 235–252, <https://doi.org/10.1002/ceat.201700327>.

[61] M.A. Aroon, A.F. Ismail, M.M. Montazer-Rahmati, T. Matsuura, Effect of chitosan as a functionalization agent on the performance and separation properties of polyimide/multi-walled carbon nanotubes mixed matrix flat sheet membranes, *J. Membr. Sci.* 364 (1) (2010) 309–317, <https://doi.org/10.1016/j.memsci.2010.08.023>.

[62] V. Nafisi, M.-B. Hägg, Development of dual layer of ZIF-8/PEBAX-2533 mixed matrix membrane for CO<sub>2</sub> capture, *J. Membr. Sci.* 459 (2014) 244–255, <https://doi.org/10.1016/j.memsci.2014.02.002>.

[63] A.K. Zulhairun, A.F. Ismail, T. Matsuura, M.S. Abdullah, A. Mustafa, Asymmetric mixed matrix membrane incorporating organically modified clay particle for gas separation, *Chem. Eng. J.* 241 (2014) 495–503, <https://doi.org/10.1016/j.cej.2013.10.042>.

[64] C. Zhang, Y. Dai, J.R. Johnson, O. Karvan, W.J. Koros, High performance ZIF-8/6FDA-DAM mixed matrix membrane for propylene/propane separations, *J. Membr. Sci.* 389 (2012) 34–42, <https://doi.org/10.1016/j.memsci.2011.10.003>.

[65] G. Liu, L. Cheng, G. Chen, F. Liang, G. Liu, W. Jin, Pebax-based membrane filled with two-dimensional MXene nanosheets for efficient CO<sub>2</sub> capture, *Chem. Asian J.* 15 (2020) 2364–2370, <https://doi.org/10.1002/asia.201901433>.

[66] J. Sun, Q. Li, G. Chen, J. Duan, G. Liu, W. Jin, MOF-801 incorporated PEBA mixed-matrix composite membranes for CO<sub>2</sub> capture, *Sep Purif. Technol.* 217 (2019) 229–239, <https://doi.org/10.1016/j.seppur.2019.02.036>.

[67] Y. Hua, H. Wang, Q. Li, G. Chen, G. Liu, J. Duan, W. Jin, Highly efficient CH<sub>4</sub> purification by LaBTB PCP-based mixed matrix membranes, *J. Mater. Chem. A* 6 (2) (2018) 599–606, <https://doi.org/10.1039/C7TA07261A>.

[68] N.A.H. Md. Nordin, A.F. Ismail, A. Mustafa, R.S. Murali, T. Matsuura, Utilizing low ZIF-8 loading for an asymmetric PSf/ZIF-8 mixed matrix membrane for CO<sub>2</sub>/CH<sub>4</sub> separation, *Rsc Adv.* 5 (38) (2015) 30206–30215, <https://doi.org/10.1039/C5RA00567A>.

[69] K. Zahri, K.C. Wong, P.S. Goh, A.F. Ismail, Graphene oxide/polysulfone hollow fiber mixed matrix membranes for gas separation, *Rsc Adv.* 6 (92) (2016) 89130–89139, <https://doi.org/10.1039/C6RA16820E>.

[70] G. Liu, V. Chernikova, Y. Liu, K. Zhang, Y. Belmabkhout, O. Shekhah, C. Zhang, S. Yi, M. Eddaoudi, W.J. Koros, Mixed matrix formulations with MOF molecular sieving for key energy-intensive separations, *Nat. Mater.* 17 (3) (2018) 283–289, <https://doi.org/10.1038/s41563-017-0013-1>.

[71] M. Etcheberry-Benavides, T. Johnson, S. Cao, B. Zornoza, J. Coronas, J. Sanchez-Lainez, A. Sabetghadam, X. Liu, E. Andres-Garcia, F. Kapteijn, J. Gascon, O. David, PBI mixed matrix hollow fiber membrane: Influence of ZIF-8 filler over H<sub>2</sub>/CO<sub>2</sub> separation performance at high temperature and pressure, 116347–116354, *Sep Purif. Technol.* 237 (2020), <https://doi.org/10.1016/j.seppur.2019.116347>.

[72] F. Pazani, M. Shariatifar, M. Salehi Maleh, T. Alebrahim, H. Lin, Challenge and promise of mixed matrix hollow fiber composite membranes for CO<sub>2</sub> separations, 122876–122897, *Sep Purif. Technol.* 308 (2023), <https://doi.org/10.1016/j.seppur.2022.122876>.

[73] G.X. Dong, H.Y. Li, V.K. Chen, Challenges and opportunities for mixed-matrix membranes for gas separation, *J. Mater. Chem. A* 1 (15) (2013) 4610–4630, <https://doi.org/10.1039/c3ta00927k>.

[74] M.R.A. Hamid, H.-K. Jeong, Recent advances on mixed-matrix membranes for gas separation: opportunities and engineering challenges, *Korean J. Chem. Eng.* 35 (8) (2018) 1577–1600, <https://doi.org/10.1007/s11814-018-0081-1>.

[75] M.A. Aroon, A.F. Ismail, T. Matsuura, M.M. Montazer-Rahmati, Performance studies of mixed matrix membranes for gas separation: a review, *Sep Purif. Technol.* 75 (3) (2010) 229–242, <https://doi.org/10.1016/j.seppur.2010.08.023>.

[76] J.R.J. Ryan Adams, Chen Zhang, Ryan Lively, Ying Dai, Omoyen Esekhele, Junqiang Liu, William J. Koros, Mixed-matrix membranes, in: V.V.T.E.M. Hoek (Ed.), *Encyclopedia of Membrane Science and Technology*, Wiley, Hoboken, 2013, pp. 1–34.

[77] S. Park, W.R. Kang, H.T. Kwon, S. Kim, M. Seo, J. Bang, Sh Lee, H.K. Jeong, J. S. Lee, The polymeric upper bound for N<sub>2</sub>/NF<sub>3</sub> separation and beyond; ZIF-8 containing mixed matrix membranes, *J. Membr. Sci.* 486 (2015) 29–39, <https://doi.org/10.1016/j.memsci.2015.03.030>.

[78] J.A. Thompson, K.W. Chapman, W.J. Koros, C.W. Jones, S. Nair, Sonication-induced Ostwald ripening of ZIF-8 nanoparticles and formation of ZIF-8/polymer composite membranes, *Microporous Mesoporous Mater.* 158 (2012) 292–299, <https://doi.org/10.1016/j.micromeso.2012.03.052>.

[79] K. Xie, Q. Fu, G.G. Qiao, P.A. Webley, Recent progress on fabrication methods of polymeric thin film gas separation membranes for CO<sub>2</sub> capture, *J. Membr. Sci.* 572 (2019) 38–60, <https://doi.org/10.1016/j.memsci.2018.10.049>.

[80] K. Yang, Y. Dai, X. Ruan, W. Zheng, X. Yang, R. Ding, G. He, Stretched ZIF-8@GO flake-like fillers via pre-Zn(II)-doping strategy to enhance CO<sub>2</sub> permeation in mixed matrix membranes, *J. Membr. Sci.* 601 (2020) 117934, <https://doi.org/10.1016/j.memsci.2020.117934>.

[81] P. Burmann, B. Zornoza, C. Téllez, J. Coronas, Mixed matrix membranes comprising MOFs and porous silicate fillers prepared via spin coating for gas separation, *Chem. Eng. Sci.* 107 (2014) 66–75, <https://doi.org/10.1016/j.ces.2013.12.001>.

[82] N.A.B. Fauzan, H.A. Mannan, R. Nasir, D.F.B. Mohshim, H. Mukhtar, Various techniques for preparation of thin-film composite mixed-matrix membranes for CO<sub>2</sub> separation, *Chem. Eng. Technol.* 42 (12) (2019) 2608–2620, <https://doi.org/10.1002/ceat.201800520>.

[83] S.H. Chaki, K.S. Mahato, T.J. Malek, M.P. Deshpande, CuAlS<sub>2</sub> thin films – Dip coating deposition and characterization, *J. Sci. Adv. Mater. Devices* 2 (2) (2017) 215–224, <https://doi.org/10.1016/j.jsamd.2017.04.002>.

[84] H. Fan, Q. Shi, H. Yan, S. Ji, J. Dong, G. Zhang, Simultaneous spray self-assembly of highly loaded ZIF-8-PDMS nanohybrid membranes exhibiting exceptionally high Biobutanol-permselective pervaporation, *Angew. Chem. Int. Ed.* 53 (22) (2014) 5578–5582, <https://doi.org/10.1002/anie.201309534>.

[85] S.A. Mohammed Rasool Qtashat, Novel techniques for preparing multi-layer polymeric and mixed matrix membranes and a device for membrane distillation, *Europe* (2014).

[86] F. Weigelt, P. Georgopanos, S. Shishatskiy, V. Filiz, T. Brinkmann, V. Abetz, Development and characterization of defect-free Matrimid® mixed-matrix membranes containing activated carbon particles for gas separation, *Polymers* 10 (1) (2018) 51–71, <https://doi.org/10.3390/polym10010051>.

[87] R. Nasir, H. Mukhtar, Z. Man, D.F. Mohshim, Material advancements in fabrication of mixed-matrix membranes, *Chem. Eng. Technol.* 36 (5) (2013) 717–727, <https://doi.org/10.1002/ceat.201200734>.

[88] J. Liu, T.-H. Bae, W. Qiu, S. Husain, S. Nair, C.W. Jones, R.R. Chance, W.J. Koros, Butane isomer transport properties of 6FDA-DAM and MFI-6FDA-DAM mixed matrix membranes, *J. Membr. Sci.* 343 (1) (2009) 157–163, <https://doi.org/10.1016/j.memsci.2009.07.018>.

[89] M. Askari, T.-S. Chung, Natural gas purification and olefin/paraffin separation using thermal cross-linkable co-polyimide/ZIF-8 mixed matrix membranes, *J. Membr. Sci.* 444 (2013) 173–183, <https://doi.org/10.1016/j.memsci.2013.05.016>.

[90] L.F. Francis, Chapter 3 - Melt Processes, in: L.F. Francis (Ed.), *Materials Processing*, Academic Press, Boston, 2016, pp. 105–249.

[91] J.-J. Kim, T.-S. Jang, Y.-D. Kwon, U.Y. Kim, S.S. Kim, Structural study of microporous polypropylene hollow fiber membranes made by the melt-spinning and cold-stretching method, *J. Membr. Sci.* 93 (3) (1994) 209–215, [https://doi.org/10.1016/0376-7388\(94\)00070-0](https://doi.org/10.1016/0376-7388(94)00070-0).

[92] F.J. Wei, H.J. Shao, B. Wu, K.Z. Zhang, D.J. Luo, S.H. Qin, Z. Hao, Effect of spin-draw rate and stretching ratio on polypropylene hollow fiber membrane made by melt-spinning and stretching method, *Int Polym. Process* 33 (1) (2018) 13–19, <https://doi.org/10.3139/217.3303>.

[93] K. Shahidi, D. Rodriguez, Production of composite membranes by coupling coating and melt extrusion/salt leaching, *Ind. Eng. Chem. Res* 56 (5) (2017) 1306–1315, <https://doi.org/10.1021/acs.iecr.6b04362>.

[94] Z. Razzaz, D. Rodriguez, Hollow fiber porous nanocomposite membranes produced via continuous extrusion: morphology and gas transport properties, *Materials* 11 (11) (2018) 2311–2330, <https://doi.org/10.3390/ma1112311>.

[95] C. Covarrubias, R. Quijada, Preparation of aluminophosphate/polyethylene nanocomposite membranes and their gas permeation properties, *J. Membr. Sci.* 358 (1) (2010) 33–42, <https://doi.org/10.1016/j.memsci.2010.04.026>.

[96] A. Kathuria, M.G. Abiad, R. Auras, Deterioration of metal-organic framework crystal structure during fabrication of poly(l-lactic acid) mixed-matrix

membranes, *Cal Poly* 62 (8) (2013) 1144–1151, <https://doi.org/10.1002/pi.4478>.

[97] H. Kim, A.A. Abdala, C.W. Macosko, Graphene/polymer nanocomposites, *Macromolecules* 43 (16) (2010) 6515–6530, <https://doi.org/10.1021/ma100572e>.

[98] S. Sinha Ray, M. Okamoto, Polymer/layered silicate nanocomposites: a review from preparation to processing, *Prog. Polym. Sci.* 28 (11) (2003) 1539–1641, <https://doi.org/10.1016/j.progpolymsci.2003.08.002>.

[99] B. Adak, M. Joshi, B.S. Butola, Polyurethane/clay nanocomposites with improved helium gas barrier and mechanical properties: Direct versus master-batch melt mixing route, *J. Appl. Polym. Sci.* 135 (27) (2018) 46422, <https://doi.org/10.1002/app.46422>.

[100] M. Fasihi, M.R. Abolghasemi, Oxygen barrier and mechanical properties of masterbatch-based PA6/nanoclay composite films, *J. Appl. Polym. Sci.* 125 (2012) E2–E8, <https://doi.org/10.1002/app.35467>.

[101] A. Zhu, A. Cai, J. Zhang, H. Jia, J. Wang, PMMA-grafted-silica/PVC nanocomposites: Mechanical performance and barrier properties, *J. Appl. Polym. Sci.* 108 (4) (2008) 2189–2196, <https://doi.org/10.1002/app.27863>.

[102] H. Kim, C.W. Macosko, Morphology and Properties of Polyester/Exfoliated Graphite Nanocomposites, *Macromolecules* 41 (9) (2008) 3317–3327, <https://doi.org/10.1021/ma702385h>.

[103] H. Kim, C.W. Macosko, Processing-property relationships of polycarbonate/graphene composites, *Polymer* 50 (15) (2009) 3797–3809, <https://doi.org/10.1016/j.polymer.2009.05.038>.

[104] J. Jin, R. Rafiq, Y.Q. Gill, M. Song, Preparation and characterization of high performance of graphene/nylon nanocomposites, *Eur. Polym. J.* 49 (9) (2013) 2617–2626, <https://doi.org/10.1016/j.eurpolymj.2013.06.004>.

[105] Y. Cui, S.I. Kundalwal, S. Kumar, Gas barrier performance of graphene/polymer nanocomposites, *Carbon* 98 (2016) 313–333, <https://doi.org/10.1016/j.carbon.2015.11.018>.

[106] P. Maiti, K. Yamada, M. Okamoto, K. Ueda, K. Okamoto, New polylactide/layered silicate nanocomposites: Role of organoclays, *Chem. Mater.* 14 (11) (2002) 4654–4661, <https://doi.org/10.1021/cm020391b>.

[107] S. Sinha Ray, K. Yamada, M. Okamoto, A. Ogami, K. Ueda, New polylactide/layered silicate nanocomposites. 3. High-performance biodegradable materials, *Chem. Mater.* 15 (7) (2003) 1456–1465, <https://doi.org/10.1021/cm020953r>.

[108] D. Rigotti, R. Checchetto, S. Tarter, D. Caretti, M. Rizzutto, L. Fambri, A. Pegoretti, Polylactic acid-lauryl functionalized nanocellulose nanocomposites: microstructural, thermo-mechanical and gas transport properties, *Express Polym. Lett.* 13 (2019) 858–876, <https://doi.org/10.3144/expresspolymlett.2019.75>.

[109] J. Han, W. Lee, J.M. Choi, R. Patel, B.-R. Min, Characterization of polyethersulfone/polyimide blend membranes prepared by a dry/wet phase inversion: precipitation kinetics, morphology and gas separation, *J. Membr. Sci.* 351 (1) (2010) 141–148, <https://doi.org/10.1016/j.memsci.2010.01.038>.

[110] S. Husain, W.J. Koros, Mixed matrix hollow fiber membranes made with modified HSSZ-13 zeolite in polyetherimide polymer matrix for gas separation, *J. Membr. Sci.* 288 (1) (2007) 195–207, <https://doi.org/10.1016/j.memsci.2006.11.016>.

[111] L.Y. Jiang, T.S. Chung, C. Cao, Z. Huang, S. Kulprathipanja, Fundamental understanding of nano-sized zeolite distribution in the formation of the mixed matrix single- and dual-layer asymmetric hollow fiber membranes, *J. Membr. Sci.* 252 (1) (2005) 89–100, <https://doi.org/10.1016/j.memsci.2004.12.004>.

[112] N. Widjojo, T.-S. Chung, Thickness and air gap dependence of macrovoid evolution in phase-inversion asymmetric hollow fiber membranes, *Ind. Eng. Chem. Res* 45 (22) (2006) 7618–7626, <https://doi.org/10.1021/ie060587>.

[113] Y. Li, T.-S. Chung, Z. Huang, S. Kulprathipanja, Dual-layer polyethersulfone (PES)/BTDA-TDI/MDI co-polyimide (P84) hollow fiber membranes with a submicron PES–zeolite beta mixed matrix dense-selective layer for gas separation, *J. Membr. Sci.* 277 (1) (2006) 28–37, <https://doi.org/10.1016/j.memsci.2005.10.008>.

[114] H. Zhu, X. Jie, L. Wang, G. Kang, D. Liu, Y. Cao, Effect of MIL-53 on phase inversion and gas separation performance of mixed matrix hollow fiber membranes, *Rsc Adv.* 6 (73) (2016) 69124–69134, <https://doi.org/10.1039/C6RA14823A>.

[115] Y. Wang, X. Wang, J. Guan, L. Yang, Y. Ren, N. Nasir, H. Wu, Z. Chen, Z. Jiang, 110th Anniversary: Mixed matrix membranes with fillers of intrinsic nanopores for gas separation, *Ind. Eng. Chem. Res* 58 (19) (2019) 7706–7724, <https://doi.org/10.1021/acs.iecr.9b00156>.

[116] H. Sun, T. Wang, Y. Xu, W. Gao, P. Li, Q.J. Niu, Fabrication of polyimide and functionalized multi-walled carbon nanotubes mixed matrix membranes by in-situ polymerization for CO<sub>2</sub> separation, *Sep Purif. Technol.* 177 (2017) 327–336, <https://doi.org/10.1016/j.seppur.2017.01.015>.

[117] L. Ma, F. Svec, T. Tan, Y. Lv, Mixed matrix membrane based on cross-linked poly [(ethylene glycol) methacrylate] and metal-organic framework for efficient separation of carbon dioxide and methane, *ACS Appl. Nano Mater.* 1 (6) (2018) 2808–2818, <https://doi.org/10.1021/acsnano.8b00459>.

[118] J. Sánchez-Lafínez, L. Paseta, M. Navarro, B. Zornoza, C. Téllez, J. Coronas, Ultrapermeable thin film ZIF-8/polyamide membrane for H<sub>2</sub>/CO<sub>2</sub> separation at high temperature without using sweep gas, 1800647–1800654, *Adv. Mater. Interfaces* 5 (19) (2018), <https://doi.org/10.1002/admi.201800647>.

[119] W.J. Lau, A.F. Ismail, N. Misdan, M.A. Kassim, A recent progress in thin film composite membrane: A review, *Desalination* 287 (2012) 190–199, <https://doi.org/10.1016/j.desal.2011.04.004>.

[120] K.C. Wong, P.S. Goh, A.F. Ismail, Thin film nanocomposite: the next generation selective membrane for CO<sub>2</sub> removal, *J. Mater. Chem. A* 4 (41) (2016) 15726–15748, <https://doi.org/10.1039/C6TA05145F>.

[121] S. Yu, S. Li, S. Huang, Z. Zeng, S. Cui, Y. Liu, Covalently bonded zeolitic imidazolate frameworks and polymers with enhanced compatibility in thin film nanocomposite membranes for gas separation, *J. Membr. Sci.* 540 (2017) 155–164, <https://doi.org/10.1016/j.memsci.2017.06.047>.

[122] K.C. Wong, P.S. Goh, B.C. Ng, A.F. Ismail, Thin film nanocomposite embedded with polymethyl methacrylate modified multi-walled carbon nanotubes for CO<sub>2</sub> removal, *Rsc. Adv.* 5 (40) (2015) 31683–31690, <https://doi.org/10.1039/C5RA00039D>.

[123] A. Awad, I.H. Aljundi, Layer-by-layer assembly of carbide derived carbon-polyamide membrane for CO<sub>2</sub> separation from natural gas, *Energy* 157 (2018) 188–199, <https://doi.org/10.1016/j.energy.2018.05.136>.

[124] H. Molavi, A. Shojaei, S.A. Mousavi, Improving mixed-matrix membrane performance via PMMA grafting from functionalized NH<sub>2</sub>-UiO-66, *J. Mater. Chem. A* 6 (6) (2018) 2775–2791, <https://doi.org/10.1039/C7TA10480D>.

[125] R. Lin, L. Ge, L. Hou, E. Stroumyna, V. Rudolph, Z. Zhu, Mixed Matrix Membranes with Strengthened MOFs/Polymer Interfacial Interaction and Improved Membrane Performance, *ACS Appl. Mater. Interfaces* 6 (8) (2014) 5609–5618, <https://doi.org/10.1021/am500081e>.

[126] N. Tien-Binh, D. Rodrigue, S. Kaliaguine, In-situ cross interface linking of PIM-1 polymer and UiO-66-NH<sub>2</sub> for outstanding gas separation and physical aging control, *J. Membr. Sci.* 548 (2018) 429–438, <https://doi.org/10.1016/j.memsci.2017.11.054>.

[127] Y. Zhang, X. Feng, H. Li, Y. Chen, J. Zhao, S. Wang, L. Wang, B. Wang, Photoinduced postsynthetic polymerization of a metal-organic framework toward a flexible stand-alone membrane, *Angew. Chem. Int. Ed.* 54 (14) (2015) 4259–4263, <https://doi.org/10.1002/anie.201500207>.

[128] S. Zhang, J. Zhang, Y. Zhang, Y. Deng, Nanoconfined ionic liquids, *Chem. Rev.* 117 (10) (2017) 6755–6833, <https://doi.org/10.1021/cr.acs.chemrev.6b00509>.

[129] B.-J. Yao, L.-G. Ding, F. Li, J.-T. Li, Y. Fu, Y. Ban, A. Guo, Y.-B. Dong, Chemically cross-linked MOF membrane generated from imidazolium-based diionic liquid-decorated UiO-66 type NMOF and its application toward CO<sub>2</sub> separation and conversion, *ACS Appl. Mater. Interfaces* 9 (44) (2017) 38919–38930, <https://doi.org/10.1021/acsmi.7b12697>.

[130] J.H. Kim, Y.M. Lee, Gas permeation properties of poly(amide-6-b-ethylene oxide)-silica hybrid membranes, *J. Membr. Sci.* 193 (2) (2001) 209–225, [https://doi.org/10.1016/S0376-7388\(01\)00514-2](https://doi.org/10.1016/S0376-7388(01)00514-2).

[131] A.M. Marti, S.R. Venna, E.A. Roth, J.T. Culp, D.P. Hopkinson, Simple fabrication method for mixed matrix membranes with in situ MOF growth for gas separation, *ACS Appl. Mater. Interfaces* 10 (29) (2018) 24784–24790, <https://doi.org/10.1021/acsmi.8b006592>.

[132] S. He, B. Zhu, X. Jiang, G. Han, S. Li, C.H. Lau, Y. Wu, Y. Zhang, L. Shao, Symbiosis-inspired de novo synthesis of ultrahigh MOF growth mixed matrix membranes for sustainable carbon capture, e2114964119–e2114964127, *PNAS* 119 (1) (2022), <https://doi.org/10.1073/pnas.2114964119>.

[133] S. Li, Y.-J. Sun, Z.-X. Wang, C.-G. Jin, M.-J. Yin, Q.-F. An, Rapid fabrication of high-permeability mixed matrix membranes at mild condition for CO<sub>2</sub> capture, 2208177–2208183, *Small* 19 (19) (2023), <https://doi.org/10.1002/smll.202208177>.

[134] Y. Hua, S. Park, G.M. Choi, H.J. Jung, K.Y. Cho, H.-K. Jeong, Highly propylene-selective asymmetric mixed-matrix membranes by polymer phase-inversion in sync with in-situ ZIF-8 formation, 143048–143055, *Chem. Eng. J.* 466 (2023), <https://doi.org/10.1016/j.cej.2023.143048>.

[135] L. Ma, F. Svec, Y. Lv, T. Tan, In situ bottom-up growth of metal-organic frameworks in a crosslinked poly(ethylene oxide) layer with ultrahigh loading and superior uniform distribution, *J. Mater. Chem. A* 7 (35) (2019) 20293–20301, <https://doi.org/10.1039/C9TA05401D>.

[136] S. Park, M.R. Abdul Hamid, H.-K. Jeong, Highly propylene-selective mixed-matrix membranes by in situ metal-organic framework formation using a polymer-modification strategy, *ACS Appl. Mater. Interfaces* 11 (29) (2019) 25949–25957, <https://doi.org/10.1021/acsmi.9b07106>.

[137] S. Park, H.-K. Jeong, In-situ linker doping as an effective means to tune zeolitic-imidazolate framework-8 (ZIF-8) fillers in mixed-matrix membranes for propylene/propane separation, 117689–117697, *J. Membr. Sci.* 596 (2020), <https://doi.org/10.1016/j.memsci.2019.117689>.

[138] S. Park, K.Y. Cho, H.-K. Jeong, Polyimide/ZIF-7 mixed-matrix membranes: understanding the in situ confined formation of the ZIF-7 phases inside a polymer and their effects on gas separations, *J. Mater. Chem. A* 8 (2020) 11210–11217, <https://doi.org/10.1039/DOTA02761H>.

[139] G. Chen, C. Chen, Y. Guo, Z. Chu, Y. Pan, G. Liu, G. Liu, Y. Han, W. Jin, N. Xu, Solid-solvent processing of ultrathin, highly loaded mixed-matrix membrane for gas separation, *Science* 381 (6664) (2023) 1350–1356, <https://doi.org/10.1126/science.adl1545>.

[140] C. Zhang, K. Zhang, L. Xu, Y. Labreche, B. Kraftschik, W.J. Koros, Highly scalable ZIF-based mixed-matrix hollow fiber membranes for advanced hydrocarbon separations, *AIChE J.* 60 (7) (2014) 2625–2635, <https://doi.org/10.1002/aijc.14496>.

[141] Y. Wang, T. Hu, H. Li, G. Dong, W. Wong, V. Chen, Enhancing membrane permeability for CO<sub>2</sub> capture through blending commodity polymers with selected PEO and PEO-PDMS copolymers and composite hollow fibres, *Energy Procedia* 63 (2014) 202–209, <https://doi.org/10.1016/j.egypro.2014.11.021>.

[142] P.C. Tan, B.S. Ooi, A.L. Ahmad, S.C. Low, Formation of a defect-free polyimide/zeolitic imidazolate framework-8 composite membrane for gas separation: in-depth analysis of organic–inorganic compatibility, *J. Chem. Technol. Biotechnol.* 94 (9) (2019) 2792–2804, <https://doi.org/10.1002/jctb.5908>.

[143] Y. Zhang, Q. Shen, J. Hou, P.D. Sutrisna, V. Chen, Shear-aligned graphene oxide laminate/Pebax ultrathin composite hollow fiber membranes using a facile dip-

coating approach, *J. Mater. Chem. A* 5 (17) (2017) 7732–7737, <https://doi.org/10.1039/C6TA10395B>.

[144] P.D. Sutrisna, J. Hou, M.Y. Zulkifli, H. Li, Y. Zhang, W. Liang, M. Deanna, V. D'Alessandro, Chen, Surface functionalized UiO-66/Pebax-based ultrathin composite hollow fiber gas separation membranes, *J. Mater. Chem. A* 6 (3) (2018) 918–931, <https://doi.org/10.1039/C7TA07512J>.

[145] Z. Yang, Y. Zhou, Z. Feng, X. Rui, T. Zhang, Z. Zhang, *A Review on reverse osmosis and nanofiltration membranes for water purification, Polymers* (2019).

[146] Y. Ding, Perspective on gas separation membrane materials from process economics point of view, *Ind. Eng. Chem. Res* 59 (2) (2020) 556–568, <https://doi.org/10.1021/acs.iecr.9b05975>.

[147] C. Astorino, E. De Nardo, S. Lettieri, G. Ferraro, C.F. Pirri, S. Bocchini, Advancements in gas separation for energy applications: Exploring the potential of polymer membranes with intrinsic microporosity (PIM), *Membranes* 13 (12) (2023) 930–959, <https://doi.org/10.3390/membranes13120903>.

[148] H. An, S. Park, H.T. Kwon, H.K. Jeong, J.S. Lee, A new superior competitor for exceptional propylene/propane separations: ZIF-67 containing mixed matrix membranes, *J. Membr. Sci.* 526 (2017) 367–376, <https://doi.org/10.1016/j.memsci.2016.12.053>.

[149] T.D. Bui, Y. Wong, M.R. Islam, K.J. Chua, On the theoretical and experimental energy efficiency analyses of a vacuum-based dehumidification membrane, *J. Membr. Sci.* 539 (2017) 76–87, <https://doi.org/10.1016/j.memsci.2017.05.067>.

[150] O. Tanskyi, Zeolite Membrane Water Vapor Separation for Building Air-Conditioning and Ventilation Systems, *Mechanical Engineering, Texas A & M University*, 2015.

[151] N. Prasetya, N.F. Himma, P.D. Sutrisna, I.G. Wenten, B.P. Ladewig, A review on emerging organic-containing microporous material membranes for carbon capture and separation, 123575-123592, *Chem. Eng. J.* 391 (2019), <https://doi.org/10.1016/j.cej.2019.123575>.

[152] A.Y. Ku, P. Kulkarni, R. Shisler, W. Wei, Membrane performance requirements for carbon dioxide capture using hydrogen-selective membranes in integrated gasification combined cycle (IGCC) power plants, *J. Membr. Sci.* 367 (1) (2011) 233–239, <https://doi.org/10.1016/j.memsci.2010.10.066>.

[153] A.W. Thornton, D. Dubbeldam, M.S. Liu, B.P. Ladewig, A.J. Hill, M.R. Hill, Feasibility of zeolitic imidazolate framework membranes for clean energy applications, *Energy Environ. Sci.* 5 (6) (2012) 7637–7646, <https://doi.org/10.1039/C2EE21743K>.

[154] R.J. Gardner, R.A. Crane, J.F. Hannan, Hollow fiber permeator for separating gases, *Chem. Eng. Prog.* 73 (1977) 76–78.

[155] M.K.T. Jay M.S. Henis, Multicomponent membranes for gas separations, *United States*, 1977.

[156] O.C. David, D. Gorri, A. Urtiaga, I. Ortiz, Mixed gas separation study for the hydrogen recovery from H<sub>2</sub>/CO/N<sub>2</sub>/CO<sub>2</sub> post combustion mixtures using a Matrimid membrane, *J. Membr. Sci.* 378 (1) (2011) 359–368, <https://doi.org/10.1016/j.memsci.2011.05.029>.

[157] L. Li, R. Xu, C. Song, B. Zhang, Q. Liu, T. Wang, A Review on the progress in nanoparticle/C hybrid CMS membranes for gas separation, *Membranes* 8 (4) (2018) 134, <https://doi.org/10.3390/membranes8040134>.

[158] R.S. Murali, T. Sankarshana, S. Sridhar, Air separation by polymer-based membrane technology, *Sep Purif. Rev.* 42 (2) (2013) 130–186, <https://doi.org/10.1080/15422119.2012.686000>.

[159] R.W. Baker, Future directions of membrane gas separation technology, *Ind. Eng. Chem. Res* 41 (6) (2002) 1393–1411, <https://doi.org/10.1021/ie0108088>.

[160] J. Ploegmakers, A.R.T. Jelsma, A.G.J. van der Ham, K. Nijmeijer, Economic evaluation of membrane potential for ethylene/ethane separation in a retrofitted hybrid membrane-distillation plant using unisim design, *Ind. Eng. Chem. Res* 52 (19) (2013) 6524–6539, <https://doi.org/10.1021/ie400737s>.

[161] G.H. Craig Colling, John Bartels, Processes using solid perm-selective membranes in multiple groups for simultaneous recovery of specified products from a fluid mixture, *United States*, 2002.

[162] H.R. Amedi, M. Aghajani, Economic estimation of various membranes and distillation for propylene and propane separation, *Ind. Eng. Chem. Res* 57 (12) (2018) 4366–4376, <https://doi.org/10.1021/acs.iecr.7b04169>.

[163] P.Z. Moghadam, A. Li, S.B. Wiggins, A. Tao, A.G.P. Maloney, P.A. Wood, S. C. Ward, D. Fairén-Jimenez, Development of a cambridge structural database subset: a collection of metal-organic frameworks for past, present, and future, *Chem. Mater.* 29 (7) (2017) 2618–2625, <https://doi.org/10.1021/acs.chemmater.7b00441>.

[164] W. Yang, H. Liang, F. Peng, Z. Liu, J. Liu, Z. Qiao, Computational screening of metal-organic framework membranes for the separation of 15 gas mixtures, *Nanomaterials* 9 (3) (2019) 467–479, <https://doi.org/10.3390/nano9030467>.

[165] Z. Qiao, Q. Xu, J. Jiang, High-throughput computational screening of metal-organic framework membranes for upgrading of natural gas, *J. Membr. Sci.* 551 (2018) 47–54, <https://doi.org/10.1016/j.memsci.2018.01.020>.

[166] S. Keskin, S. Alsayo Altinkaya, A Review on computational modeling tools for MOF-based mixed matrix membranes, *Computation* 7 (3) (2019) 36–61, <https://doi.org/10.3390/computation7030036>.

[167] A. Ebneyamini, H. Azimi, F.H. Tezel, J. Thibault, Mixed matrix membranes applications: development of a resistance-based model, *J. Membr. Sci.* 543 (2017) 351–360, <https://doi.org/10.1016/j.memsci.2017.08.065>.

[168] B. Shimekit, H. Mukhtar, T. Murugesan, Prediction of the relative permeability of gases in mixed matrix membranes, *J. Membr. Sci.* 373 (1) (2011) 152–159, <https://doi.org/10.1016/j.memsci.2011.02.038>.

[169] R. Pal, New models for thermal conductivity of particulate composites, *J. Reinf. Plast. Compos* 26 (7) (2007) 643–651, <https://doi.org/10.1177/0731684407075569>.